nature metabolism

ARTICLES

https://doi.org/10.1038/s42255-021-00364-0

Check for updates

Pre-existing beta cells but not progenitors contribute to new beta cells in the adult pancreas

Huan Zhao[1], Xiuzhen Huang[1], Zixin Liu[1], Wenjuan Pu[1], Zan Lv[1], Lingjuan He[1], Yan Li[1], Qiao Zhou[2], Kathy O. Lui[3] and Bin Zhou[1,4,5,6] ✉

It has been suggested that new beta cells can arise from specific populations of adult pancreatic progenitors or facultative stem cells. However, their existence remains controversial, and the conditions under which they would contribute to new beta-cell formation are not clear. Here, we use a suite of mouse models enabling dual-recombinase-mediated genetic tracing to simultaneously fate map insulin-positive and insulin-negative cells in the adult pancreas. We find that the insulin-negative cells, of both endocrine and exocrine origin, do not generate new beta cells in the adult pancreas during homeostasis, pregnancy or injury, including partial pancreatectomy, pancreatic duct ligation or beta-cell ablation with streptozotocin. However, non-beta cells can give rise to insulin-positive cells after extreme genetic ablation of beta cells, consistent with transdifferentiation. Together, our data indicate that pancreatic endocrine and exocrine progenitor cells do not contribute to new beta-cell formation in the adult mouse pancreas under physiological conditions.

Insulin-secreting pancreatic beta cells are central to the proper maintenance of whole-body glucose homeostasis. Normal glycaemic control requires an adequate number of functional beta cells; consequently, beta-cell death is a pathological hallmark of type 1 diabetes and advanced type 2 diabetes[1,2]. The ability of functional beta cells to regulate real-time glycaemic control, and thus the avoidance of chronic organ damage, far exceeds the capability of exogenous insulin treatment. Therefore, there is an increasing demand for therapeutic approaches that restore functional and effective beta-cell mass in patients with severe beta-cell deficiency[3]. Understanding how endogenous beta cells are generated during homeostasis and potentially in disease conditions would provide clinically relevant information for designing new therapeutic approaches to treat diabetes. Regarding the identification of the cellular sources for generating new beta cells in the adult pancreas, to date, two distinct mechanisms have been reported: self-replication of pre-existing beta cells and generation of new beta cells from non-beta cells[4]. In support of the first mechanism, several pioneering studies using genetic lineage tracing elegantly demonstrated that beta-cell replication is the predominant means by which new beta cells are generated after birth and in response to injury in vivo[5–8]. The second proposed mechanism regarding the generation of new beta cells in the adult could occur by either transdifferentiation of differentiated non-beta cells or differentiation of pancreatic stem or progenitor cells (termed neogenesis).

Non-beta cells of the adult human pancreas are capable of beta-cell differentiation when co-transplanted with fetal pancreatic cells under the mouse kidney capsule[9]. Adult glucagon-producing alpha cells and somatostatin-producing delta cells can transdifferentiate into new beta cells after extreme beta-cell loss (>99%) mediated by diphtheria toxin (DT)-based genetic ablation[10,11]. Forced overexpression of the transcription factor Pax4 or selective inhibition of Arx in mouse alpha cells is sufficient to promote their conversion to beta cells[12,13]. Expression of Pdx1 and Mafa endows human alpha cells with beta-cell characteristics[14]. Beyond this transdifferentiation of endocrine cells, expression of the key beta-cell developmental regulators neurogenin 3 (Neurog3), Pdx1 and Mafa, can reprogramme adult mouse exocrine cells into cells that closely resemble beta cells[15]. Similarly, the acinar-cell-specific expression of Pdx1 also converts adult exocrine cells into insulin-expressing beta cells[16]. Notably, many of the above studies supporting transdifferentiation utilized forced gene expression and used genetic tracing to demonstrate direct conversion of differentiated cells into insulin-producing beta cells. Under these specific non-physiological conditions, as mentioned above, new beta cells could be derived from other non-beta-cell lineages.

While there is a consensus regarding the transdifferentiation pathway for adult beta-cell regeneration, whether beta-cell neogenesis exists in the adult pancreas under physiological conditions remains controversial. Several lineage-tracing studies have supported the existence of facultative beta-cell progenitors or stem cells that differentiate into beta cells after pancreatic injury. For instance, adult ductal Neurog3-expressing cells, which have been reported as progenitors of beta cells, can be reactivated autonomously to proliferate and differentiate into beta cells after injury in a pancreatic duct ligation (PDL) model[17]. Adult carbonic anhydrase II–positive cells of the pancreatic duct may also serve as progenitors and give rise to beta cells after PDL[18]. Similarly, a small number of adult Ptf1a$^+$ acinar cells could undergo rapid reprogramming to generate duct cells and produce a small number of insulin-positive beta cells after PDL[19]. Additional studies have also suggested the existence of pancreatic stem cells or progenitors, including CD133$^+$ cells[20], Aldh1a1$^+$ cells[21], Pdx1$^+$ cells[22], Sox9$^+$ ductal cells[23] and the recently reported Procr$^+$ cells[24]. Contrary to these studies, a large body of evidence

[1]State Key Laboratory of Cell Biology, Shanghai Institute of Biochemistry and Cell Biology, Center for Excellence in Molecular Cell Science, Chinese Academy of Sciences; University of Chinese Academy of Sciences, Shanghai, China. [2]Division of Regenerative Medicine, Department of Medicine, Weill Cornell Medical College of Cornell University, New York, NY, USA. [3]Department of Chemical Pathology; Li Ka Shing Institute of Health Sciences, Prince of Wales Hospital, The Chinese University of Hong Kong, Hong Kong, China. [4]School of Life Science and Technology, ShanghaiTech University, Shanghai, China. [5]School of Life Science, Hangzhou Institute for Advanced Study, University of Chinese Academy of Sciences, Hangzhou, China. [6]Institute for Stem Cell and Regeneration, Chinese Academy of Sciences, Beijing, China. ✉e-mail: zhoubin@sibs.ac.cn

from lineage-tracing studies that relied on a variety of exocrine and endocrine markers does not support the stem cell hypothesis for beta-cell neogenesis[25–29]. Due to the conflicting nature of these studies, there remains much debate and contention over the role of stem cells in beta-cell neogenesis.

In this study, we reassessed the stem cell hypothesis by developing a dual-recombinase-mediated genetic system, in which pre-existing insulin-positive beta cells and all insulin-negative non-beta cells, including putative stem and progenitor cells, are simultaneously labelled by distinct surrogate markers that enable indelible tracing. With this dual fate-mapping approach, we found that non-beta cells generate new beta cells in the adult pancreas during embryogenesis but not during homeostasis, pregnancy or after various forms of injuries, including partial pancreatectomy (PPX), PDL and beta-cell ablation with streptozotocin (STZ). However, formation of new insulin-positive cells from insulin-negative cells was observed after DT-mediated extreme beta-cell loss, consistent with direct transdifferentiation from alpha and delta cells. Thus, while our study supports the idea that beta-cell self-replication is the dominant pathway for beta-cell regeneration in the adult mouse pancreas, there is no evidence for beta-cell neogenesis.

Results

Generation of fate-mapping system to track beta and non-beta cells. To genetically label all putative beta-cell progenitors and stem cells without relying on prior knowledge of specific markers, we developed a dual genetic-fate-mapping system for simultaneous labelling of insulin-producing beta cells and all non-beta cells (Fig. 1a). In the construct design, we used two orthogonal site-specific recombination systems, Cre-loxP and Dre-rox, with an interleaved reporter, *IR1* (refs. [30–33]). In the *IR1* reporter, two pairs of recombination recognition sites (rox and loxP) were interleaved, such that one successful recombination resulted in expression of one distinct genetic reporter and prevented any further event from another type of recombination. For example, Dre-rox recombination in beta cells first removes the rox-flanked segment that contains one loxP site and ZsGreen from *IR1*, such that this allele would then express tdTomato (tdT) and would no longer be responsive to Cre-loxP recombination (Fig. 1a). Likewise, Cre-loxP recombination in non-beta cells removes the loxP-flanked segment that contains one rox site and the transcriptional stop cassette for ZsGreen expression, preventing subsequent Dre-rox-mediated recombination. Recombination is prevented even if this non-beta cell (for example, a stem cell) could later differentiate into an insulin-producing beta cell. This design would thus simultaneously label beta cells and non-beta cells with two distinct permanent surrogate markers, tdT and ZsGreen, respectively (Fig. 1a). If authentic beta-cell progenitors or stem cells exist and contribute to new beta cells, the newly differentiated insulin-producing beta cells would be genetically traced by ZsGreen expression.

To label insulin-producing beta cells, we first generated the *Ins2-Dre* knock-in line by targeting the Dre recombinase cDNA located directly after the endogenous insulin gene promoter. The ATG start codon was replaced by homologous recombination using CRISPR–Cas9 (Extended Data Fig. 1a). By crossing the mouse line with *IR1*, *Ins2-Dre* efficiently labelled insulin-expressing beta cells, rendering virtually all beta cells positive for tdT in the adult islets (Extended Data Fig. 1), and thus demonstrated the high efficiency of genetic targeting to insulin-expressing beta cells. We next generated an inducible Cre system, *R26-iCre*, consisting of *R26-rtTA* and *TRE-Cre* alleles. In this system, doxycycline (Dox)-mediated rtTA binding to TRE leads to Cre expression, which recombines with the *IR1* allele and yields constitutively active expression of ZsGreen (Fig. 1b).

We treated 6-week-old *Ins2-Dre;R26-iCre;IR1* mice with Dox for 1 week and analysed non-beta-cell labelling a week later (Fig. 1c). Whole-mount fluorescence imaging of the pancreas from the 7-week-old Dox-treated mice showed tdT$^+$ islets peppered within ZsGreen$^+$ signal (Fig. 1d), while no ZsGreen$^+$ signal was observed in the pancreas without Dox treatment (Fig. 1e). Immunostaining for tdT, ZsGreen and insulin (Ins) on pancreatic sections derived from the Dox-treated *Ins2-Dre;R26-iCre;IR1* mice showed that virtually all Ins$^+$ beta cells were positive for tdT (Fig. 1f,h). For examination of ZsGreen$^+$ cells in dual lineage-tracing models, multiple regions of immunostained pancreatic tissue sections were randomly selected for image collection and quantification of the percentage of labelled cells. In the whole-pancreas sections with magnification of multiple regions, we found all regions randomly selected were highly efficient in ZsGreen labelling (Extended Data Fig. 2). Examination of the different endocrine cell lineages of islets showed broad ZsGreen expression in non-beta-cell lineages, such as alpha cells (94.95% ± 1.22%), delta cells (92.52% ± 0.86%) and pancreatic polypeptide cells (97.79% ± 0.36%; Extended Data Fig. 3). In the exocrine tissues, ZsGreen were also broadly expressed in multiple non-beta cells, such as acinar cells (98.58% ± 0.28%), ductal cells (97.20% ± 0.57%), endothelial cells (95.72% ± 1.08%), lymphatic endothelial cells (94.58% ± 0.86%) and fibroblasts (93.26% ± 0.73%; Extended Data Fig. 4). Quantitatively, 96.30% ± 1.38% of non-beta cells expressed ZsGreen (ZsGreen$^+$tdT$^-$DAPI$^+$/tdT$^-$DAPI$^+$), demonstrating that the vast majority of non-beta cells were labelled by *R26-iCre* (Fig. 1f,h). In the control group lacking Dox treatment, beta cells were positive for tdT, and non-beta cells remained negative for ZsGreen (Fig. 1g,h). By these means, we developed a genetic system marked by tdT$^+$ beta cells and ZsGreen$^+$ non-beta cells in the mouse pancreas (Fig. 1i).

Assessment of beta-cell neogenesis during homeostasis. To test whether non-beta cells could contribute to beta-cell neogenesis during homeostasis, we treated 6-week-old *Ins2-Dre;R26-iCre;IR1* mice with Dox for 1 week, followed by analyses at 3 or 6 months after induction (Fig. 2a). We performed whole-mount fluorescence imaging of pancreas samples at these two time points and found a strong ZsGreen$^+$ signal throughout the entire pancreas coupled with isolated speckles of tdT$^+$ staining (Fig. 2b). Next, we immunostained pancreatic tissue sections at these two time points for tdT, ZsGreen and Ins, and found that all beta cells maintained islet-specific tdT expression (Fig. 2c–e). We did not find any cells co-expressing ZsGreen and insulin in the pancreatic tissues at both time points (Fig. 2c–e). All Ins$^+$ cells exclusively expressed tdT, but none of them expressed ZsGreen (Fig. 2d,e). These fate-mapping data indicate that insulin-negative endocrine or exocrine cells did not give rise to new beta cells in the adult pancreas under homeostatic conditions (Fig. 2f).

Prior studies have reported that multipotent endocrine progenitors exist in the embryonic and fetal pancreas, which can give rise to insulin-producing beta cells[25–27,34]. To test if our system could track beta-cell generation during embryogenesis, we collected pancreas samples from *Ins2-Dre;R26-iCre;IR1* mice at embryonic day (E) 14.5 without Dox treatment and confirmed the presence of Ins$^+$tdT$^+$ cells (Extended Data Fig. 5a). We then performed pulse–chase experiments by treating *Ins2-Dre;R26-iCre;IR1* mice with Dox at E14.5 and collecting the pancreas at E16 and postnatal day (P) 21 to compare the ZsGreen labelling rate of beta cells. By genetic design, the *IR1* allele could be recombined by one type of recombinase only and then permanently expressed afterwards. The pre-existing beta cells would be labelled by *Ins2-Dre* (tdT), non-beta cells including stem cells or progenitors would be labelled by inducible Cre after Dox treatment (ZsGreen), and their descendants including beta cells would be permanently ZsGreen$^+$. As more beta cells arise from ZsGreen$^+$ progenitors or stem cells over time during embryonic development, the tdT labelling rate of beta cells would be expected to be diluted, while the ZsGreen labelling rate of beta cells would

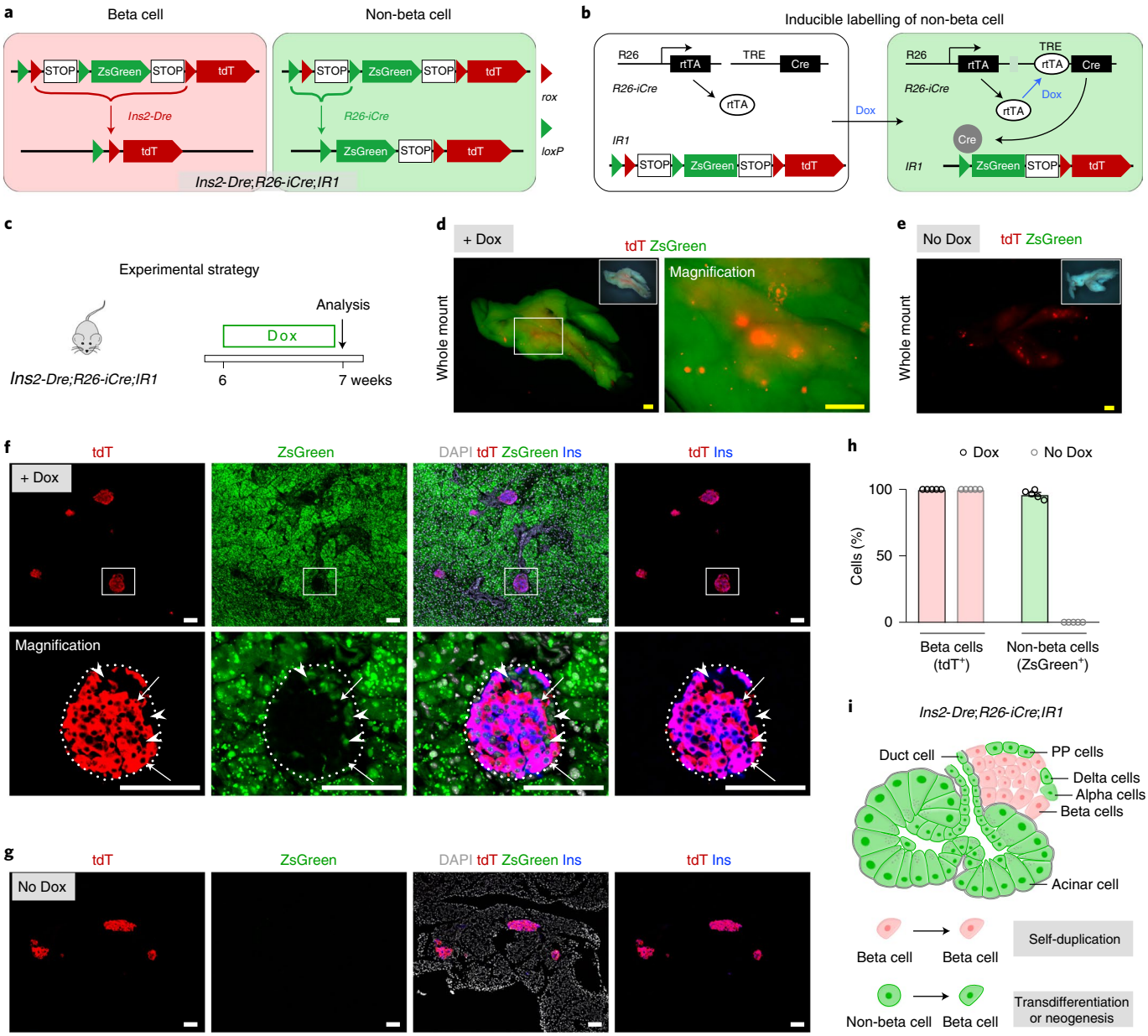

Fig. 1 | Genetic labelling of beta cells and non-beta cells by a *Ins2-Dre;R26-iCre;IR1* strategy. a, Schematic illustrating the strategy for labelling pancreatic beta cells and non-beta cells by the *Ins2-Dre;R26-iCre;IR1* model using a dual-recombinase-based genetic approach. **b**, Schematic illustrating the means by which Dox induces the labelling of non-beta cells by Cre-loxP-mediated recombination via the *R26-rtTA;TRE-Cre* (*R26-iCre*) model. **c**, Schematic illustrating the experimental strategy for Dox-induced lineage tracing of beta and non-beta cells. Male and female mice aged 6 weeks were treated with ($n=5$) or without ($n=5$) Dox for 1 week before euthanization. **d**,**e**, Whole-mount fluorescence images of pancreas from indicated mice with (**d**) or without (**e**) Dox treatment. Inserts show bright-field images of pancreas. **f**,**g**, Immunostaining for tdT, ZsGreen and Ins on pancreatic slides collected from *Ins2-Dre;R26-iCre;IR1* mice treated with Dox (**f**) or no Dox (**g**). Arrows indicate tdT$^+$Ins$^+$ beta cells. Arrowheads indicate ZsGreen$^+$Ins$^-$ non-beta cells. **h**, Quantification of the percentage of beta cells expressing tdT or non-beta cells expressing ZsGreen from *Ins2-Dre;R26-iCre;IR1* mice treated with Dox or without Dox. Pancreas samples from individual mice were examined in each group: Dox, $n=5$; no Dox, $n=5$. Data are the mean ± s.e.m. **i**, Illustration showing the dual labelling of beta cells and non-beta cells in *Ins2-Dre;R26-iCre;IR1* mice. PP, pancreatic polypeptide. Scale bars: 1 mm (yellow); 100 μm (white). Each image is representative of five individual biological samples.

be expected to increase over time. By examining the tissue sections stained with ZsGreen, tdT and Ins, we found the ZsGreen labelling rate of beta cells was 9.46% ± 0.52% at E16 and increased to 27.14% ± 1.51% at P21 ($P=1.12\times10^{-4}$; Extended Data Fig. 5b–e). However, we did not observe Ins$^+$ZsGreen$^+$ beta cells in the islets when Dox was administered postnatally after P7 (Extended Data Fig. 5f–j). These findings are consistent with previous studies showing that endocrine progenitors give rise to new beta cells during embryogenesis, but not postnatally[25–27,34]. These data also provide technical controls supporting the ability of our dual genetic tracing strategy to detect the conversion of non-beta cells to beta cells, if any exists.

Non-beta cells do not convert to beta cells during partial pancreatectomy or pregnancy. To test whether non-beta cells contribute to adult beta cells under physiological conditions known

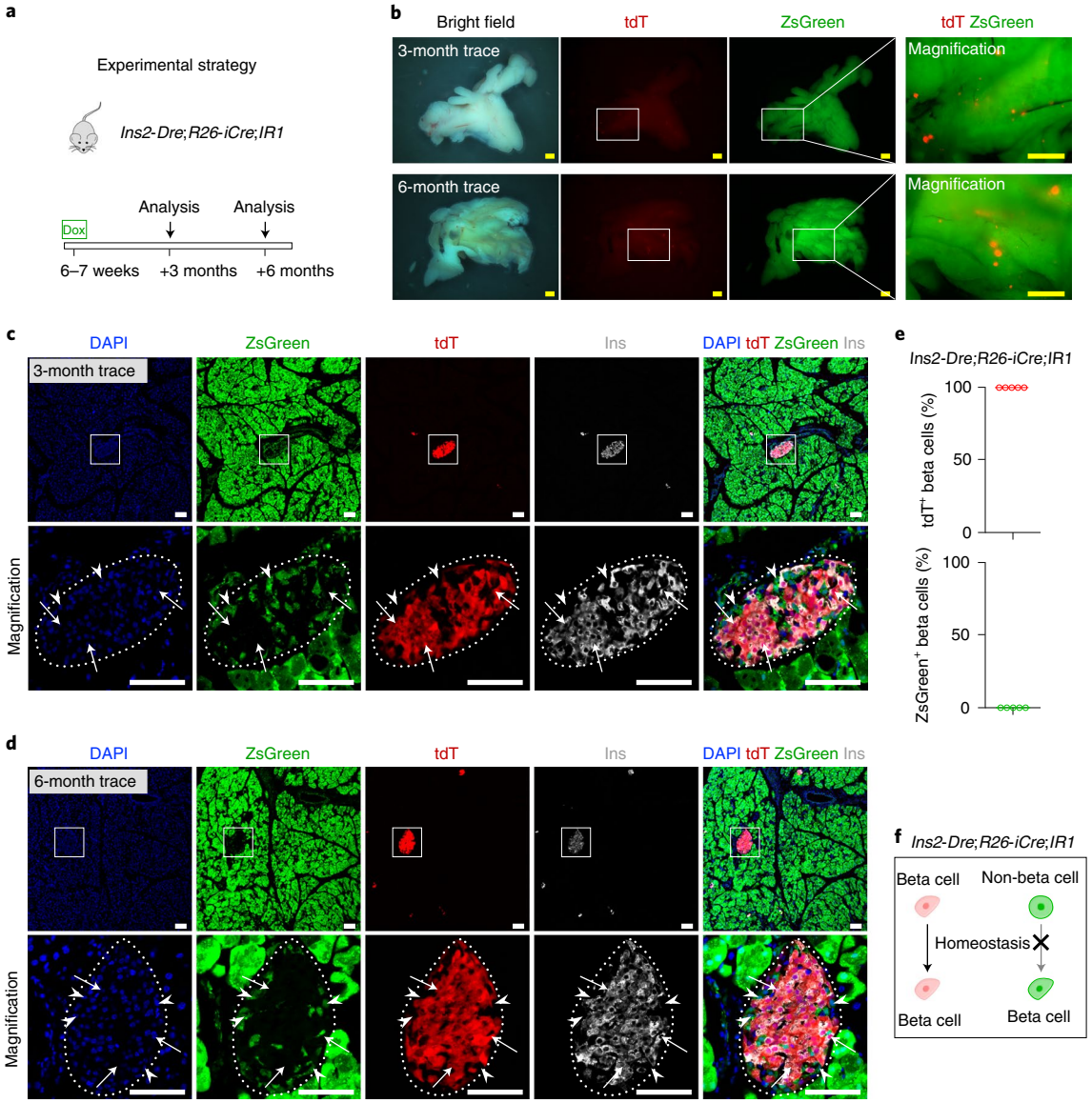

Fig. 2 | Non-beta cells do not contribute to beta cells during adult homeostasis. a, Schematic illustrating the experimental strategy to test for beta-cell neogenesis during homeostasis. Male and female mice aged 6 weeks were treated with Dox for 1 week. After 3 or 6 months, mice were euthanized (3-month trace group: $n=5$; 6-month trace group: $n=5$). **b**, Whole-mount bright-field and fluorescence images showing pancreas from *Ins2-Dre;R26-iCre;IR1* mice after 3 or 6 months of lineage tracing. **c**,**d**, Immunostaining for tdT, ZsGreen and Ins on pancreatic slides collected from *Ins2-Dre;R26-iCre;IR1* mice after 3 (**c**) or 6 (**d**) months. Arrows indicate tdT$^+$Ins$^+$ beta cells. Arrowheads indicate ZsGreen$^+$Ins$^-$ non-beta cells. **e**, Quantification of the percentage of beta cells expressing tdT or ZsGreen after 6 months of lineage tracing. Pancreas samples from individual mice were examined: $n=5$ (6-month trace group), Data are the mean ± s.e.m. **f**, Illustration showing that non-beta cells do not differentiate into beta cells during homeostasis. Scale bars: 1 mm (yellow); 100 μm (white). Each image is representative of five individual biological samples.

to stimulate beta-cell proliferation, we used a previously described PPX model to induce tissue regeneration[29]. We treated 6-week-old *Ins2-Dre;R26-iCre;IR1* mice with Dox for 1 week, performed 50% PPX after 2 weeks of washout and collected pancreatic tissue at 1, 2 and 4 weeks after injury (Fig. 3a and Extended Data Fig. 6a). We performed whole-mount fluorescence imaging and found readily detectable tdT$^+$ islets in the pancreas after PPX (Fig. 3b). The newly regenerated pancreatic tissues included both islets and exocrine cells (Fig. 3c). Immunostaining for tdT, ZsGreen and insulin on pancreatic sections also confirmed that all beta cells were positive for tdT, but none expressed ZsGreen in both the sham and PPX groups (Fig. 3d–f and Extended Data Fig. 6b,d). In line with previous studies[5,7,35,36], we found increased incorporation of EdU in the islets of PPX samples compared with sham controls (1.99% ± 0.10% in PPX versus 0.45% ± 0.05% in controls; $P=1.22\times10^{-5}$; Extended Data Fig. 6c). Of note, we found that a few tdT$^+$ cells in the islets were negative for insulin, possibly indicating beta-cell dedifferentiation as previous described[37–39]. These data demonstrate that PPX did not lead to beta-cell formation from non-beta cells (Fig. 3g).

We next asked if non-beta cells contribute to adult beta cells throughout pregnancy, during which a notable increase of beta-cell mass occurs[40]. We treated 6-week-old *Ins2-Dre;R26-iCre;IR1* mice with Dox for 1 week, set up mating after 2 weeks of washout and examined pancreatic tissues at day 15.5 of pregnancy (Fig. 3h). We found that islets of pregnant dams exhibited a robust generation of new beta cells as demonstrated by a large number of

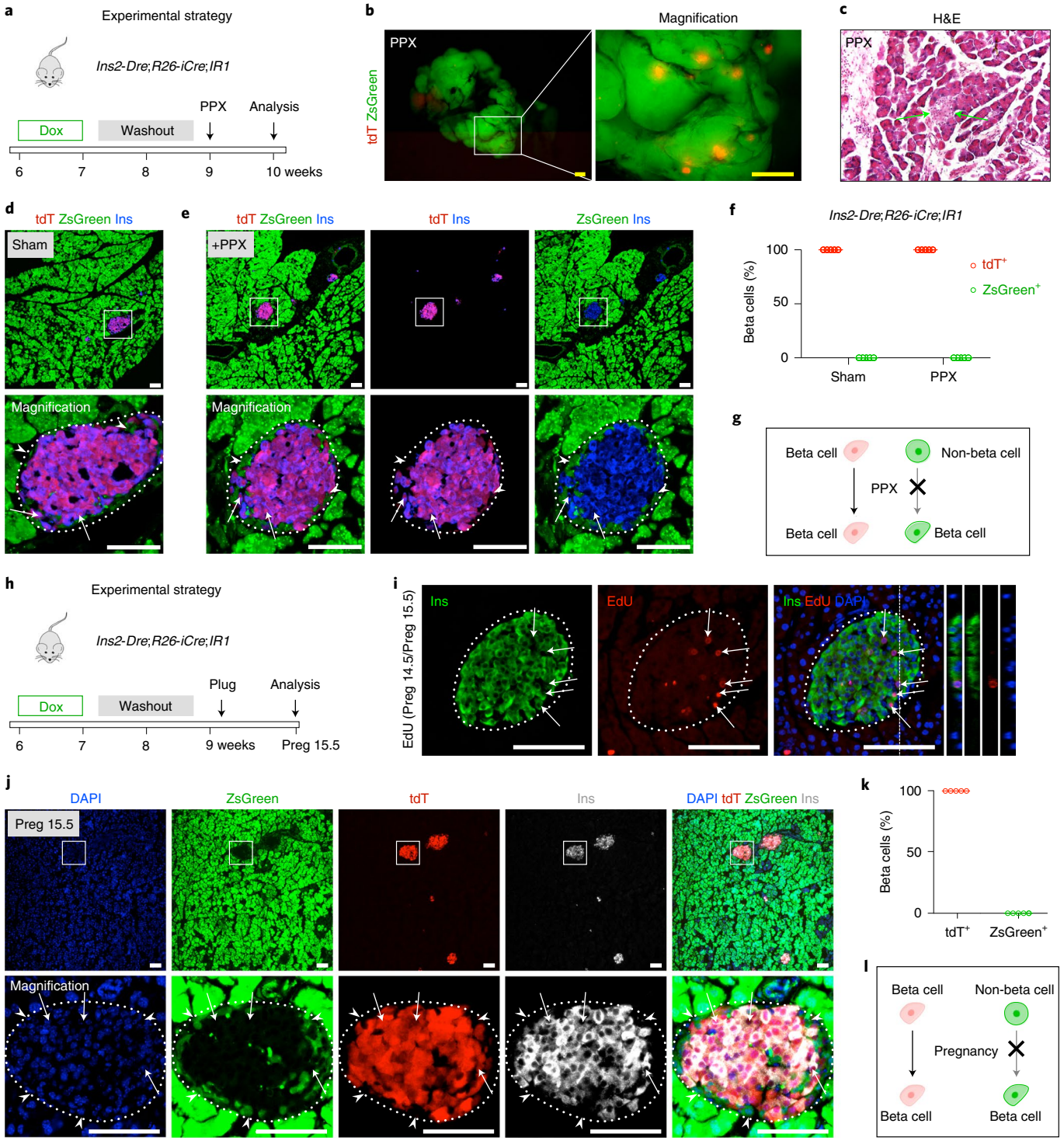

Fig. 3 | Non-beta cells do not contribute to beta cells during partial pancreatectomy and pregnancy. a, Schematic illustrating the experimental strategy to test for beta-cell neogenesis after PPX-induced injury. Male and female mice aged 6 weeks were treated with Dox for 1 week. After washout for 2 weeks and PPX injury for 1 week, mice were euthanized (PPX: $n=5$; sham: $n=5$). **b**, Whole-mount fluorescence images of pancreas from PPX mice. **c**, H&E staining of pancreatic sections collected from mice after PPX-induced njury. Arrows, islet. **d**,**e**, Immunostaining for tdT, ZsGreen and Ins on pancreatic slides collected from *Ins2-Dre;R26-iCre;IR1* sham (**d**) or PPX (**e**) mice. Arrows indicate tdT$^+$Ins$^+$ beta cells. Arrowheads indicate ZsGreen$^+$Ins$^-$ non-beta cells. **f**, Quantification of the percentage of beta cells expressing tdT or ZsGreen. Numbers of mice in each group were: sham, $n=5$; PPX, $n=5$. Data are the mean ± s.e.m. **g**, Illustration showing no contribution of non-beta cells to beta cells after PPX. **h**, Schematic illustrating the experimental strategy to test for beta-cell neogenesis during pregnancy. Female mice aged 6 weeks were treated with Dox for 1 week. After washout for 2 weeks and pregnancy for 15.5 d, mice were euthanized (pregnancy group: $n=5$; sham group: $n=5$). **i**, Immunostaining for Ins and EdU on pancreatic sections collected from mice at day 15.5 of pregnancy (preg 15.5) after EdU injection at day 14.5 (Preg 14.5). Arrows indicate EdU$^+$Ins$^+$ beta cells. **j**, Immunostaining for tdT, ZsGreen and Ins on pancreatic sections collected from *Ins2-Dre;R26-iCre;IR1* mice after pregnancy. Arrows indicate tdT$^+$Ins$^+$ beta cells. Arrowheads indicate ZsGreen$^+$Ins$^-$ non-beta cells. **k**, Quantification of the percentage of beta cells expressing tdT or ZsGreen. Pregnancy group, $n=5$ mice. Data are the mean ± s.e.m. **l**, Illustration showing no contribution of non-beta cells to beta cells during pregnancy. Scale bars: 1 mm (yellow); 100 μm (white). Each image is representative of five individual biological samples.

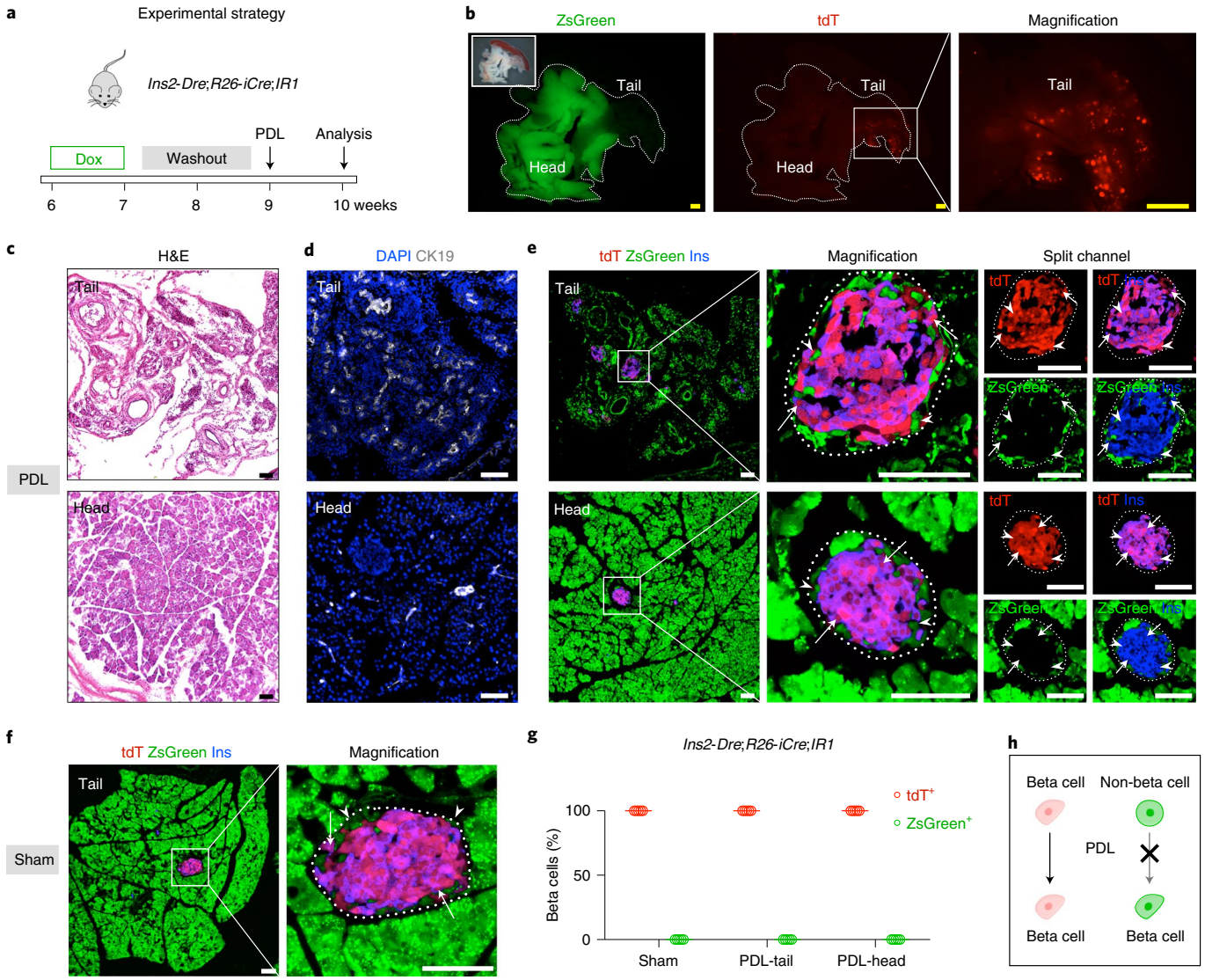

Fig. 4 | Non-beta cells do not give rise to new beta cells after pancreatic duct ligation–induced injury. a, Schematic illustrating the experimental strategy to test for beta-cell neogenesis after PDL. Male and female mice aged 6 weeks were treated with Dox for 1 week. After washout for 2 weeks and PDL injury for 1 week, mice were euthanized (PDL group: $n=5$; sham group: $n=5$). **b**, Whole-mount fluorescence images of pancreas from indicated mice 1 week after PDL injury. Insert shows a bright-field image. **c**, H&E staining of sections from the tail and the head of the pancreas after PDL. **d**, Immunostaining for CK19 of sections from the tail and the head of the pancreas after PDL. **e**, Immunostaining for tdT, ZsGreen and Ins from pancreatic tail and head sections collected after PDL. Arrows indicate tdT$^+$Ins$^+$ beta cells. Arrowheads indicate ZsGreen$^+$Ins$^-$ non-beta cells. **f**, Immunostaining for tdT, ZsGreen and Ins of pancreatic tail sections collected from sham mice. Arrows indicate tdT$^+$Ins$^+$ beta cells. Arrowheads indicate ZsGreen$^+$Ins$^-$ non-beta cells. **g**, Quantification of the percentage of beta cells expressing tdT or ZsGreen in pancreas from sham and PDL mice. Numbers of mice in each group were: sham, $n=5$; PDL-tail, $n=5$; PDL-head, $n=5$. Data are the mean ± s.e.m. **h**, Illustration showing no contribution of non-beta cells to beta cells after PDL injury. Scale bars: 1 mm (yellow); 100 µm (white). Each image is representative of five individual biological samples.

EdU-expressing beta cells during pregnancy (Fig. 3i and Extended Data Fig. 6e,f; 3.67% ± 0.14% in pregnancy versus 0.41% ± 0.05% in controls; $P=3.38\times10^{-6}$). Immunostaining for tdT, ZsGreen and ins on pancreatic sections revealed that all beta cells expressed tdT, but not ZsGreen (Fig. 3j,k). The ZsGreen$^+$ cells detected in the pancreas were exocrine cells and non-beta cells of the islets (Fig. 3j). Extrapolating from these findings, our data suggest that no beta-cell neogenesis occurs from progenitors or stem cells after PPX or during pregnancy (Fig. 3l).

Non-beta cells do not contribute to adult beta cells after pancreatic duct ligation. As previous studies have reported that PDL triggers Ins$^-$ progenitor cells to differentiate into new beta cells[17–19], we next induced PDL in 9-week-old *Ins2-Dre;R26-iCre;IR1* mice after 1 week of Dox treatment that started at 6 weeks of age and was followed by a 2-week washout period (Fig. 4a). Loss of acinar cells in the ligated tail of the pancreas gave the region a more translucent appearance within 1 week after PDL (Fig. 4b). The islets in the tail section of the pancreas could be seen clearly with the naked eye (Fig. 4b). H&E staining also showed severe inflammation and atrophy in the exocrine tissues of the tail section, but not the head, of the pancreas (Fig. 4c), with a marked increase of CK19$^+$ ductal cells in the injured tail (Fig. 4d). Immunostaining for tdT, ZsGreen and insulin revealed that ZsGreen$^+$ cells did not express insulin, and all Ins$^+$ beta cells in both the head and tail of the pancreas were positive for tdT within 1, 2 and 4 weeks after PDL (Fig. 4e and Extended Data

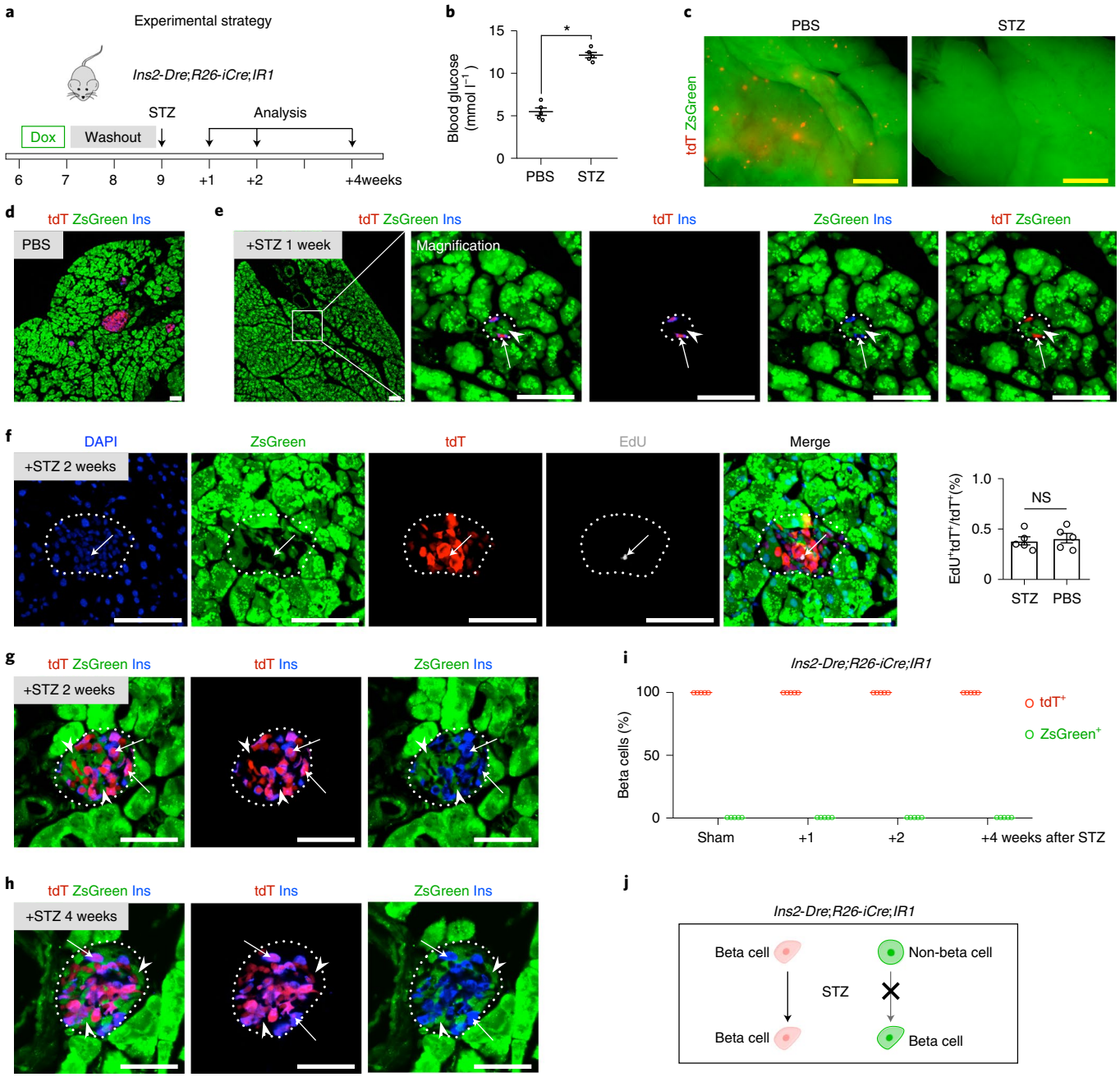

Fig. 5 | Non-beta cells do not generate new beta cells during streptozotocin-induced beta-cell loss. a, A schematic illustrating the experimental strategy to test for beta-cell neogenesis after STZ-induced injury. Male and female mice aged 6 weeks were treated with Dox for 1 week. After washout for 2 weeks and STZ injury for 1, 2 and 4 weeks, mice were euthanized (sham, $n=5$; +1 week, $n=5$; +2 weeks, $n=5$; +4 weeks, $n=5$). **b**, Detection of fasting blood glucose levels in the STZ group and the control group treated with phosphate-buffered saline (PBS) after 1 week. Numbers of mice examined were: PBS, $n=5$; STZ, $n=5$. Data are the mean ± s.e.m.; $P=3.32\times10^{-6}$, $^*P<0.05$ (unpaired, two-sided, Student's *t*-test). **c**, Whole-mount fluorescence images of pancreatic tissue for tdT$^+$ islets after STZ treatment, compared with those from the PBS group. **d**,**e**, Immunostaining of pancreatic sections for tdT, ZsGreen and Ins on pancreatic slides collected from *Ins2-Dre;R26-iCre;IR1* mice 1 week after treatment with PBS (**d**) and STZ (**e**). Arrows indicate tdT$^+$Ins$^+$ beta cells. Arrowheads indicate ZsGreen$^+$Ins$^-$ non-beta cells. **f**, Immunostaining on pancreatic sections for tdT, ZsGreen and EdU collected 2 weeks after STZ treatment. Arrows indicate EdU$^+$tdT$^+$cells. EdU was injected 12 h before euthanization. Right, quantification of the percentage of tdT$^+$ cells with incorporated EdU. Numbers of mice examined were: PBS, $n=5$; STZ, $n=5$. Data are the mean ± s.e.m.; $P=0.69$; NS, not significant (unpaired, two-sided Student's *t*-test). **g**,**h**, Immunostaining of pancreatic sections for tdT, ZsGreen and Ins on pancreatic slides collected from *Ins2-Dre;R26-iCre;IR1* mice at 2 weeks (**g**) and 4 weeks (**h**) after STZ injection. Arrows indicate tdT$^+$Ins$^+$ beta cells. Arrowheads indicate ZsGreen$^+$Ins$^-$ non-beta cells. **i**, Quantification of the percentage of beta cells expressing tdT or ZsGreen. Numbers of mice examined were: sham, $n=5$; +1 week, $n=5$; +2 weeks, $n=5$; +4 weeks, $n=5$. Data are the mean ± s.e.m. **j**, Illustration showing no contribution of non-beta cells to beta cells during STZ-induced injury. Scale bars: 1 mm (yellow); 100 μm (white). Each image is representative of five individual biological samples.

Fig. 7). In the model of PDL-induced injuries, we did not detect a significant increase in beta-cell generation compared with that of controls (Extended Data Fig. 7c; $P=0.63$). Of note, the expression levels of insulin among these tdT$^+$ cells were not homogeneous; some cells expressed a weak level of insulin in the islets (Fig. 4e). We did not detect any ZsGreen$^+$ cells expressing insulin in the sham group, similarly to the PDL group (Fig. 4f,g). Altogether, our results showed no obvious beta-cell neogenesis after PDL, consistent with previous works[27,36] (Fig. 4h).

No evidence of beta-cell neogenesis after streptozotocin-mediated injury. To test whether beta-cell loss as a result of diabetes may trigger the conversion of non-beta cells to beta cells, we treated *Ins2-Dre;R26-iCre;IR1* mice with a single injection of beta-cell-specific toxin STZ intraperitoneally following 1 week of Dox administration and then analysed the pancreas samples from these mice at 1, 2 or 4 weeks after depletion (Fig. 5a). As expected, STZ-treated mice exhibited significantly higher fasting blood glucose levels (5.50 ± 0.43 mmol l^{-1} versus 12.14 ± 0.33 mmol l^{-1}; $P=3.32\times10^{-6}$; Fig. 5b), and they displayed reduced tdT expression in the islets compared with that in controls, as demonstrated by whole-mount fluorescence imaging (Fig. 5c). Immunostaining for tdT, ZsGreen and insulin on the pancreatic sections showed a striking loss of Ins$^+$ beta cells 1 week after STZ treatment compared to those in the controls (Fig. 5d,e). In samples collected 2 and 4 weeks after STZ treatment, we observed more Ins$^+$ beta cells in the islets compared with the samples collected 1 week after STZ treatment (Fig. 5g,h), possibly indicating a slow recovery of beta cells after a severe degree of beta-cell death (Fig. 5f; $P=0.69$). However, these Ins$^+$ cells did not express ZsGreen (Fig. 5i), excluding their non-beta-cell origins. These data show lack of beta-cell neogenesis in the adult pancreas following STZ-induced beta-cell injury (Fig. 5j).

Non-beta cells generate insulin-positive cells after extreme beta-cell loss. To provide a further technical control to demonstrate the capability of the dual-tracing system in detecting the conversion of non-beta cells to beta cells, we developed an iterated version of the *IR1* mouse line with the diphtheria toxin receptor (DTR), *IR1-DTR* (Extended Data Fig. 8a). Immunostaining on pancreatic sections of *Ins2-Dre;IR1-DTR* mice for ZsGreen, tdT, insulin and DTR showed specific expression of tdT and DTR, but not ZsGreen, in Ins$^+$ beta cells (Extended Data Fig. 8b–d). DT (10 μg g^{-1} daily × 2 d) treatment led to a significant reduction of tdT$^+$ beta cells compared to those in the control group without DT (Extended Data Fig. 8e–h). However, there were some cells that expressed DTR but not tdT, which could be due to variation in the protein degradation rate of tdT and DTR in these cells within 2 d after DT treatment. We confirmed that the tdT and DTR were colocalized in beta cells without DT treatment (Extended Data Fig. 8g,h). After we successfully generated the *IR1-DTR* line, we crossed it with *Ins2-Dre* and *R26-iCre* mice to trace beta cells and non-beta cells after genetic ablation of beta cells by treatment with DT (10 μg g^{-1} daily × 5 d) after Dox-mediated labelling for 1 week followed by a washout period of 2 weeks (Fig. 6a,b). Immunostaining for ZsGreen, tdT and insulin of pancreatic sections showed a notably lower number of tdT$^+$ beta cells in the DT treatment group compared to that in the control (Fig. 6c). Over 99% of tdT$^+$ beta cells were genetically ablated, which was also confirmed by immunostaining for DTR$^+$ beta cells (Fig. 6d). The remaining cells of the islets were largely non-beta cells, such as glucagon-producing alpha cells and somatostatin-producing delta cells (Fig. 6e).

We next analysed the pancreas 4 weeks after DT treatment to determine whether new beta cells could be regenerated from non-beta cells over time. Immunostained pancreatic sections for ZsGreen, tdT and insulin showed reappearance of Ins$^+$ beta cells at 4 weeks after DT treatment (Fig. 6f). Most of these newly formed Ins$^+$ beta cells were positive for ZsGreen, indicating that they originated from pre-labelled ZsGreen$^+$ non-beta cells (917 Ins$^+$ beta cells from 191 islets in sections; $n=5$; Fig. 6f). Quantification of the percentage of Ins$^+$ beta cells expressing tdT or ZsGreen showed that while all Ins$^+$ beta cells in the control mice were tdT$^+$ZsGreen$^-$ cells, the majority of Ins$^+$ beta cells were positive for ZsGreen with a minority expressing dT after DT treatment (Fig. 6f). To further evaluate these newly generated insulin-positive cells, we performed immunostaining of other beta-cell markers with tdT and ZsGreen and found that some ZsGreen$^+$tdT$^-$ cells in the islet expressed other hallmarks of beta cells, including Pdx1, GLUT2 and Nkx6.1 (Fig. 6g). While ~80% of Ins$^+$tdT$^-$ZsGreen$^+$ cells expressed glucagon and somatostatin, ~20% of Ins$^+$tdT$^-$ZsGreen$^+$ cells lost glucagon and somatostatin expression at 4 weeks after DT treatment, suggesting both existence of bi-hormonal cells and formation of mono-hormonal beta cells in this genetic system. (Fig. 6h). The results from the mice at 4 weeks after DT treatment demonstrated that our dual-tracing genetic system was able to detect the conversion of non-beta cells to beta cells in the adult pancreas, if any exist (Fig. 6i).

Inducible saturated tracing of beta cells reveals no neogenesis. It is possible that *Ins2-Dre* could unexpectedly label very few putative stem cells that transiently express insulin at the fetal stage. In this case, these rare putative stem cells would be labelled as tdT$^+$ by *Ins2-Dre;IR1*, escaping non-beta-cell labelling as ZsGreen$^+$ by *R26-iCre;IR1*. Labelling beta cells at a specific time window with an inducible method avoids the caveat caused by the constitutive activation of Dre. We adopted the elegant strategy of lineage tracing at saturation of cell labelling, as reported previously[41], to reassess beta-cell regeneration in the adult pancreas. In this design, almost every single Ins$^+$ beta cell is genetically labelled by insulin-inducible recombinase at a given time after tamoxifen treatment. When Ins$^+$ beta cells express a reporter, such as tdT, other non-beta cells that contain the putative beta-cell progenitors do not express insulin and become negative for tdT. After the pulse–chase period, if tdT$^-$ stem

Fig. 6 | Non-beta cells contribute to insulin-positive cells after genetic ablation of beta cells. a, Schematic illustrating the experimental strategy to test for beta-cell neogenesis after severe loss of beta-cell mass. Male and female mice aged 6 weeks were treated with Dox for 1 week. After washout for 2 weeks and DT injury for 2 weeks and 4 weeks, mice were euthanized (+2 weeks, $n=5$; +2 weeks sham, $n=5$; +4 weeks, $n=5$; +4 weeks sham, $n=5$). **b**, Whole-mount bright-field and fluorescence images of pancreas from *Ins2-Dre;R26-iCre;IR1-DTR* mice at 2 weeks after DT or no DT. **c**, Immunostaining of pancreatic sections for tdT, ZsGreen and Ins at 2 weeks after DT or no DT. Right, quantification of insulin-positive beta-cell number per islet sections. Numbers of mice examined were: no DT, $n=5$; DT, $n=5$. Data are the mean ± s.e.m. **d**, Immunostaining of pancreatic sections for tdT, ZsGreen and DTR at 2 weeks after DT or no DT. **e**, Immunostaining of pancreatic sections for tdT, ZsGreen, glucagon (GCG) and somatostatin (Stt) at 2 weeks after DT or no DT. **f**, Immunostaining of pancreatic sections for tdT, ZsGreen and Ins at 4 weeks after DT or no DT. Right, quantification of the percentage of insulin-positive cells expressing tdT or ZsGreen in DT or no DT groups. Numbers of examined mice in each group were: no DT, $n=5$; DT, $n=5$. Data are the mean ± s.e.m. Arrowheads indicate ZsGreen$^+$Ins$^+$ beta cells. **g**, Immunostaining for tdT, ZsGreen, Pdx1, GLUT2 and Nkx6.1 on pancreatic sections at 4 weeks after DT. **h**, Immunostaining for tdT, ZsGreen, GCG, Stt and Ins on pancreatic sections at 4 weeks after DT. **i**, Schematic showing that non-beta cells can contribute to Ins$^+$ cells after genetic ablation of beta cells. Scale bars: 1 mm (yellow); 100 μm (white). Each image is representative of five individual samples.

cells differentiate into new beta cells, they would start to express insulin. However, these newly formed Ins$^+$ beta cells would remain as tdT$^-$ cells, as there is no tamoxifen at this stage to activate the insulin-specific inducible recombinase. The efficacy of this strategy in addressing beta-cell sources largely depends on the efficiency of labelling beta cells by the inducible recombinase. In theory, every pre-existing beta cell is labelled if the efficiency is 100%; therefore, any new beta cell differentiated from a putative stem cell would be observed as an Ins$^+$tdT$^-$ beta cell. If the efficiency of beta-cell labelling is not 100% but very close to 100% (for example, >99.9%), the newly formed Ins$^+$tdT$^-$ beta cells differentiated from putative stem cells could be recorded when the percentage of tdT$^-$ beta cells increases significantly over 0.1%. Therefore, the accuracy in interpretation using this system requires an insulin-specific inducible recombinase line with super efficiency.

To address this requirement, we first tested the labelling efficiency of a previously reported inducible Cre line, *Rip-CreER*[5], and found that it labelled a substantial portion of beta cells after

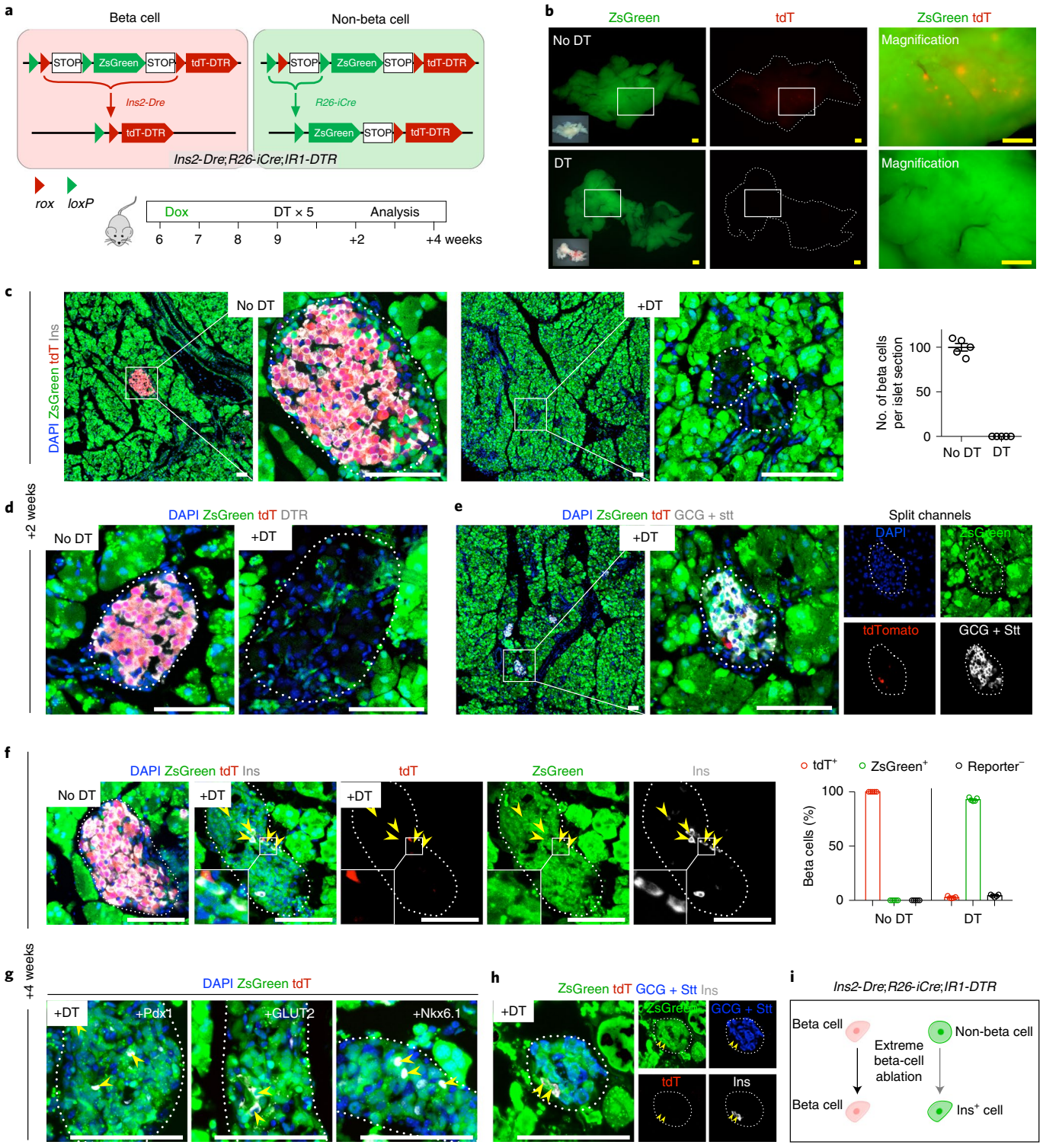

tamoxifen induction. Although efficient, we aimed to reach even higher labelling saturation (that is, >99.9–100%). Consequently, we generated two new mouse lines: an insulin-specific inducible recombinase mouse line and a new responding reporter line, as both recombinase and reporter alleles influence the recombination efficiency[42]. We first generated a new *Ins2-DreER* knock-in line by inserting DreER into the insulin gene, replacing the endogenous start codon with a homologous recombination using CRISPR–Cas9 (Fig. 7a). We also generated a new rox knock-in reporter, *H11-rox-tdTomato* (Fig. 7a) by targeting the rox-stop-rox-tdT cassette on the intergenic *Hipp11* (*H11*) locus of mouse chromosome 11 (ref. [43]). By crossing *Ins2-DreER* with *H11-rox-tdT*, tamoxifen-induced Dre-rox recombination removed the stop cassette, resulting in constitutively active expression of tdT in Ins$^+$ cells (Fig. 7b). New beta cells derived from stem cells at the chasing stage would not express tdT due to the nature of the pulse–chase strategy. We injected three doses of tamoxifen, and then analysed tissue samples at 1 week or 25 weeks afterwards (Fig. 7c). Surprisingly, the adult *Ins2-Dre;H11-rox-tdTomato* mice exhibited an unprecedentedly high labelling efficiency for beta cells, albeit with the use of an inducible recombinase. We examined Ins$^+$ beta cells for >1,000 islets and found that virtually every Ins$^+$ beta cell expressed tdT (Fig. 7d and Extended Data Fig. 9). These tdT$^+$ cells were exclusively Ins$^+$ beta cells (Fig. 7d,e and Extended Data Fig. 9), demonstrating the specificity of this technique for lineage tracing of beta cells. Examination of the pancreatic tissues after 25 weeks revealed that virtually all Ins$^+$ beta cells were tdT$^+$ (>99.9%; Fig. 7f). This saturation of beta-cell labelling was not due to leakiness of DreER activity, as all Ins$^+$ beta cells were negative for tdT in the pancreas without tamoxifen treatment (Fig. 7g). Notably, we found no detectable dilution of tdT$^+$ labelling in beta cells from 1 week to 25 weeks (Fig. 7d,f), further suggesting that non-beta cells did not contribute to any detectable adult beta-cell biogenesis during tissue homeostasis.

Given the super-efficient and highly specific properties of the *Ins2-DreER* line, we next used it to reassess the possible differentiation of putative tdT$^-$ stem cells into beta cells after PPX (Fig. 7h). Whole-mount fluorescence images of the regenerated part of pancreas collected from *Ins2-DreER;H11-rox-tdT* mice showed tdT$^+$ islets (Fig. 7i). Immunostaining of pancreatic sections for tdT and insulin showed virtually all Ins$^+$ cells were tdT$^+$ after PPX (Fig. 7j). Indeed, quantification data revealed that >99.9% of Ins$^+$ cells remained positive for tdT (Fig. 7j), indicating no beta-cell neogenesis at a detectable level after PPX. We also performed other models including during pregnancy and in PDL- and STZ-induced injuries on *Ins2-DreER;H11-rox-tdT* mice, and found no beta-cell neogenesis (Extended Data Fig. 10). Together, the above results based on tracing at saturation argue against beta-cell neogenesis in the adult pancreas during homeostasis or after injury (Fig. 7k).

Discussion

In this study, we developed a new genetic lineage-tracing system to simultaneously label both the beta and non-beta-cell populations with two distinct and irreversible genetic markers in the adult mouse pancreas. Using non-genetically manipulated injury models for inducing beta-cell death, cell growth, regeneration and inflammation, we found that newly formed beta cells during repair and regeneration were derived from pre-existing beta cells, but not non-beta cells. Additionally, we adopted a strategy of lineage tracing at saturation by generating a super-efficient beta-cell labelling tool, and we confirmed that non-beta cells did not contribute to any new beta cells during homeostasis, pregnancy and after various injuries. These results suggest that stem cell differentiation is unlikely to be the mechanism for beta-cell regeneration, at least in the injury models tested in this study (Fig. 8).

The controversial conclusions regarding the existence of endogenous stem cells or progenitors for beta-cell conversion in the adult pancreas have also been drawn from genetic lineage-tracing studies. The main caveat of these lineage-tracing methods is the non-specific labelling by reporters that are supposed to be activated through Cre recombinase driven under the control of 'cell-specific' markers[44,45]. The discrepancy between studies supporting or refuting the stem cell hypothesis is at least partly due to the specificity and stability of the proposed stem cell markers used in these studies. For example, the evidence in support of Ngn3$^+$ stem cells generating new beta cells is predicated on the notion that Ngn3 is not expressed in the pre-existing beta cells[17]. Lack of Ngn3 expression in beta cells was the linchpin of this study; however, subsequent follow-up studies have revealed that Ngn3 is actually expressed by both proliferating ducts and pre-existing beta cells[29], possibly leading to data misinterpretation. Similarly, a handful of previous studies have recorded the cell fate commitment of facultative stem cells to beta cells by lineage tracing in mice, in which the data interpretation heavily relies on the specificity of the stem cell markers[17–24]. In theory, these 'stem cell markers' should not be expressed by the pre-existing Ins$^+$ beta cells. It should also be noted that a weak expression of stem cell marker genes driving Cre below the sensitivity limit for antibody detection might still induce Cre-loxP recombination in some beta cells. The antecedent weak Cre expression in beta cells could thus result in unexpected labelling of pre-existing beta cells in subsequent studies, giving rise to false-positive results and misinterpretation. Therefore, the previous conclusions about the contribution of stem cells in beta-cell neogenesis require independent reassessments to more closely scrutinize whether a low level of beta cells were pre-labelled.

Previous studies that argue against the progenitor or stem cell hypothesis mainly used inducible lineage tracing of beta cells[5], and found no statistically significant dilution of beta-cell labelling percentage in pulse–chase experiments (~30–40%), suggesting no differentiation of beta-cell progenitors. However, this strategy was

Fig. 7 | Genetic tracing of beta cells by the inducible *Ins2-DreER;H11-rox-tdT* system during homeostasis and after injury. a, Schematic illustrating the generation of *Ins2-DreER* and *H11-rox-tdT* knock-in mouse lines by homologous recombination. **b**, Schematic illustrating genetic lineage tracing of Ins$^+$ beta cells by Dre-rox recombination. **c**, Schematic illustrating the experimental strategy. Male and female mice aged 6–7 weeks were treated with tamoxifen (tam) three times. After 1 week and 25 weeks, mice were euthanized (+1 week: $n=5$ (tam), $n=5$ (no tam); +25 weeks: $n=5$ (tam) and $n=5$ (no tam)). **d**, Whole-mount fluorescence images of pancreas and immunostaining for tdT and insulin on sections from *Ins2-DreER;H11-rox-tdT* mice at 1 week after tamoxifen treatment. Right, quantification of labelling efficiency and specificity for beta cells. Data are the mean ± s.e.m.; $n=5$ (tam). **e**, Immunostaining of pancreatic sections for tdT, GCG, Stt or PP, and the quantification of each (right) indicating the percentage of tdT$^+$ cells expressing these markers. Data are the mean ± s.e.m.; $n=5$ (tam). **f**,**g**, Immunostaining for tdT and insulin on pancreatic sections collected at 25 weeks after tamoxifen (**f**) or no tamoxifen (**g**). Quantification data of labelling efficiency for beta cells. Data are the mean ± s.e.m.; $n=5$ (tam). **h**, Schematic illustrating the experimental design to test for beta-cell neogenesis after PPX in the inducible system. Male and female mice aged 6 weeks were treated with tamoxifen three times. After washout for 2 weeks and PPX injury for 2 weeks, mice were euthanized (PPX, $n=5$; no tam, $n=5$). **i**, Whole-mount fluorescence images of the regenerated pancreas (right side of the dotted line) after PPX. **j**, Immunostaining of pancreatic sections for tdT and insulin after PPX (left) and quantification of beta cells expressing tdT (right) in the groups treated with tamoxifen or no tamoxifen. Numbers of mice examined in each group were: tam, $n=5$; no tam, $n=5$. Data are the mean ± s.e.m. **k**, Illustration showing that non-beta cells do not contribute to beta cells during homeostasis and after injuries. Scale bars: 1 mm (yellow); 100 μm (white). Each image is representative of five individual samples.

based on statistical evaluation and could not exclude small contributions of beta cells from putative stem cells or progenitor cells. Another line of evidence used constitutive Cre driven by an insulin promoter and took advantage of an mTmG reporter for capturing the transient co-expression of GFP and mTomato during beta-cell neogenesis, and showed no double-fluorescence cells in adult pancreas after various models of beta-cell loss, growth and regeneration[29]. However, it is technically difficult to capture the transient stage during beta-cell differentiation, especially when very few beta cells are derived from progenitors or stem cells. Due to the above reasons, it is possible that some undifferentiated stem cells or progenitors, beyond detection by previous lineage-tracing studies, contribute to a small number of beta cells during homeostasis or injuries. In this study, we developed a dual-recombinase-mediated genetic system to label those non-beta cells and examine if they could contribute to beta cells during pancreas homeostasis and injuries. Our work is not merely confirmatory. First, this dual genetic system differs from previous studies because it tracks non-beta cells

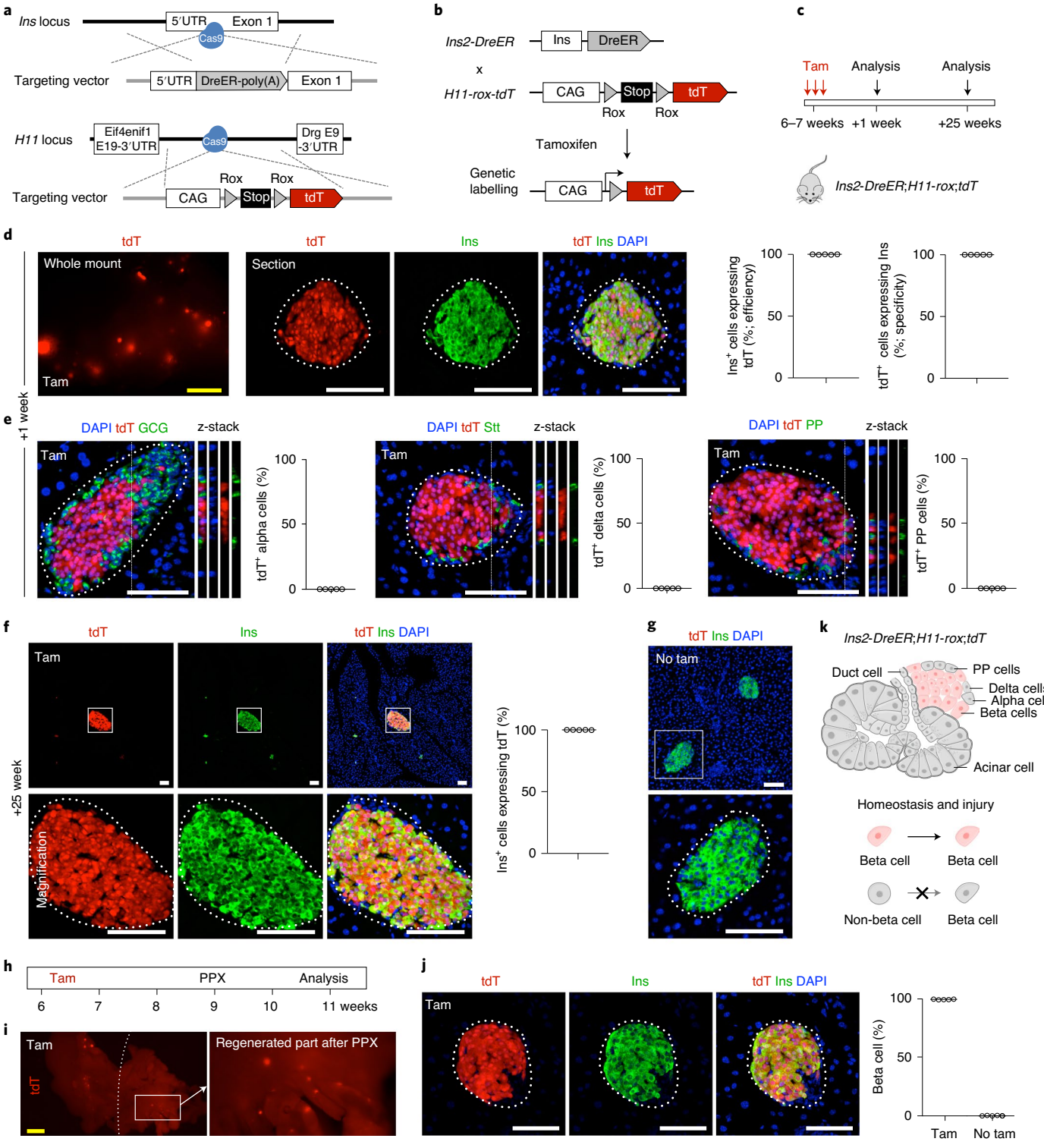

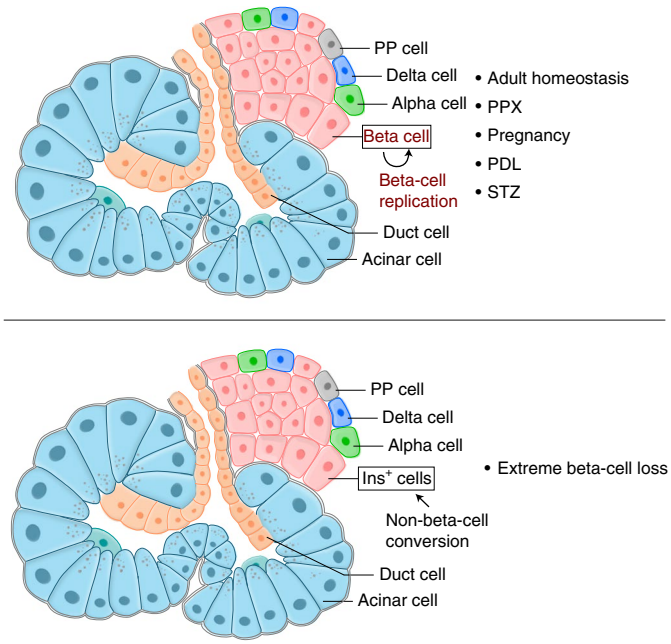

Fig. 8 | Non-beta cells do not generate new beta cells in adults under pathological conditions. Cartoon showing labelling of beta cells and non-beta cells simultaneously. Non-beta cells, including alpha cells, delta cells, PP cells, acinar cells and duct cells, do not generate new beta cells under homeostatic and pathological conditions (top). Non-beta cells do generate new Ins$^+$ cells in adults after extreme loss of existing beta cells (bottom).

permanently with a fluorescence marker, and evaluating the contribution of non-beta cells to beta cells does not rely on statistical significance, but on a single-cell basis. Even with little contribution from stem cells, if this occurs minimally (for example, <1%), we could readily detect it with positive-fluorescence lineage tracing. Second, our genetic system enables random labelling of non-beta cells using a ubiquitously active promoter, thus avoiding reliance on one particular stem cell marker. This is important as there may be putative progenitors with unknown markers residing in islets. Our genetic system allows us to examine the non-beta-cell contribution without knowing markers for stem cells. The fate-mapping results showed that non-beta cells do not generate new beta cells in the pancreas during homeostasis, pregnancy or injury. Of note, if most beta cells were genetically ablated, we could detect a small number of new beta cells arising from non-beta cells, indicating that our dual-recombinase-mediated genetic tracing system is capable of detecting beta-cell neogenesis, even if it occurs at low frequency.

In our system, most of the non-beta cells are labelled with ZsGreen (>96%), which is more efficient than any other inducible tracing strategy that we know of. The promoter of Rosa26 used in our system is widely used in genetic lineage tracing and has been shown to be ubiquitously active in tissues. The genetic labelling strategy is therefore entirely random and does not exclude any particular cell populations. Thus, any potential stem cell population, if it exists, will be labelled and detected. We used the *Ins2-Dre* knock-in line to label all Ins$^+$ beta cells as tdT$^+$ cells, and non-beta cells as ZsGreen$^+$ cells by the exclusive dual reporter *IR1*. Although all tdT$^+$ cells were positive for insulin in the initial stage, we did observe a subset of tdT$^+$ cells that expressed weak or non-existent levels of insulin after severe injuries. This was likely due to dedifferentiation of beta cells, which has been reported as a mechanism to compensate for the loss of proper beta-cell mass in different models of diabetes in mice[37]. Another possibility is that few non-beta cells at the adult stage were labelled as tdT$^+$ cells as they may have transiently expressed insulin and as such were labelled during early development by constitutive Dre. To address this issue of constitutive Dre, we used a strategy called inducible lineage tracing at saturation[41]. We unexpectedly found an inducible *Ins2-DreER* mouse line that provided a super-efficient tool after it was crossed with *H11-rox-tdTomato* to label virtually all Ins$^+$ beta cells at the adult stage. We did not see any flux or dilution of the tdT surrogate marker in beta-cell labelling during pancreatic homeostasis or after injuries, demonstrating that there was no beta-cell progenitor accounting for any detectable beta-cell neogenesis. Furthermore, transdifferentiation of non-beta cells such as alpha, delta or exocrine cells, did not contribute to adult beta cells in our non-genetically manipulated injury models. Taken together, our findings leverage the recent advances in dual-tracing genetic technology coupled with inducible lineage tracing at saturation to show that adult beta-cell regeneration is predominantly mediated by self-replication, rather than by stem or progenitor cell differentiation.

Methods

Mice. All mouse experiments were carried out in accordance with the guidelines of the Institutional Animal Care and Use Committee of the Institute of Biochemistry and Cell Biology, and the Institute for Nutritional Sciences, Shanghai Institutes for Biological Sciences, Chinese Academy of Science. Mice were maintained on a C57BL6/ICR mixed background, housed in standard cages and maintained on a 12-h light/dark cycle and fed a normal diet (Jiangsu Xietong Pharmaceutical Bioengineering, 1010085). Unless otherwise stated, both male and female heterozygote mice (6–8 weeks old) were randomly allocated to control and experimental groups. Littermate controls were used when appropriate. Only female mice were used in the pregnancy group and the sham group. *R26-rtTA*, *TRE-Cre* and *IR1* mouse lines were described previously[5,33,46–50]. *Ins2-Dre* and *Ins2-DreER* were generated using the CRISPR–Cas9 technology by Shanghai Biomodel Organism. A cDNA encoding Dre or DreER was targeted to the translational start codon ATG of the *Ins* gene by homologous recombination, replacing the endogenous translational start codon ATG, followed by woodchuck post-transcriptional regulatory element and poly(A). PCR primers, spanning the genomic DNA, were designed to test the correctly targeted allele (*Ins2-Dre*, 5′mut-F: AAGATACTAGGTCCCCAACTGCAAC, 5′mut-R: TTCAGCATGGCG TAGTGCTTGTCG, 5′WT-F: AAACAGCAAAGTCCAGGGGG, 5′WT-R: ATGG GTGTGTAGAAGAAGCCACGC; *Ins2-DreER*, 5′mut-F: GATCCGCTACAATCA AAAACCATCAGC, 5′mut-R: TCCCGGGCCTCCACC, 5′WT-F: CCTCTCTTA CGTGAAACTTTTGCTATCCTC, 5′WT-R: TCAGACAGAGGAGGCAGGCCA). *H11-rox-tdTomato* was generated using the CRISPR–Cas9 technology by Shanghai Biomodel Organism. A cDNA encoding rox-Stop-rox-tdTomato was targeted to the *Hipp11* site by homologous recombination, followed by post-transcriptional regulatory element and poly(A). PCR primers spanning the genomic DNA were designed to test the correctly targeted allele (*H11-rox-tdTomato*, 5′mut-F: CACTCTACTGGAGGAGGACAAACTG, 5′mut-R: ACAACGAGGACTACA CCATCGTG, 5′WT-F: TGGAGGAGGACAAACTGGTCAC, 5′WT-R: TTCCC TTTCTGCTTCATCTTGC). *IR1-DTR* was generated using the CRISPR–Cas9 technology by Shanghai Biomodel Organism. A cDNA encoding CAG-loxP-rox-Stop-loxP-ZsGreen-Stop-rox-tdTomato-P2A-DTR cassette was targeted to the Rosa26 site by homologous recombination. PCR primers spanning the genomic DNA were designed to test the correctly targeted allele (*IR1-DTR*, 3′mut-F: GGC ACGCTGATCTACAAGGTGAA, 3′mut-R: GTGCTTGTGGCTTGGAGGATAA, 5′WT-F: TTGGAGGCAGGAAGCACTTG, 5′WT-R: CCGACAAAACCGAAA ATCTGTG). Genomic DNA was extracted from a mouse tail snip and prepared for genotyping by proteinase K lysis, isopropanol precipitation and 70% ethanol washing. The starting points for each experiment involved 6- to 8-week-old adult mice. For adult mouse treatment, Dox was dissolved in ddH_2O (2 mg ml^{-1}) and used to feed mice for 1 week. For embryo mouse treatment, Dox was dissolved in ddH_2O (20 mg ml^{-1}) and introduced by gavage (0.1 mg g^{-1}) to pregnant mice twice in 3 d. For postnatal mouse treatment, Dox was dissolved in ddH_2O (20 mg ml^{-1}) and introduced by gavage (0.1 mg g^{-1}) twice. To assess cell proliferation, mice were injected subcutaneously with EdU (Invitrogen, C10338; 10 μg g^{-1}) dissolved in PBS 24 h or 12 h before euthanization. Tamoxifen was dissolved in corn oil (20 mg ml^{-1}) and introduced by gavage (0.1 mg g^{-1}) at the indicated time points. The beta-cell toxin STZ was dissolved as previously described[3] and introduced by intraperitoneal injection (150 mg per kg body weight). Blood glucose levels of different groups of mice were measured after a 12-h fasting period. DT was dissolved in PBS (1 μg μl^{-1}) and introduced by intraperitoneal injection (10 μg g^{-1}) per mouse, twice each to induce some beta-cell loss, and five times each to induce extreme beta-cell loss.

Partial pancreatectomy. PPX was performed as previously described[29,35]. Briefly, adult mice were anaesthetized with isoflurane gas and a midline abdominal

incision was made. The mesenteric connections to the stomach, small intestine and retroperitoneum were partially broken. The splenic lobe of the pancreas was moved and then the pancreatic tissue, bordered by the spleen and stomach, excluding the small flap of pancreatic tissue attached to the pylorus, was removed. The sham group underwent laparotomy. All mice received a standard laboratory chow diet and tap water post-operatively.

Pancreatic duct ligation. PDL was performed as previously described[29]. Briefly, adult mice were anesthetized with isoflurane gas and a midline abdominal incision was made. The duodenum and the head of the pancreas were lifted off the retroperitoneum. The pancreatic duct at the left side of the portal vein, which separates the splenic and gastro-duodenal lobes were carefully ligated. Sham group underwent laparotomy. All mice received a standard laboratory chow diet and tap water post-operatively.

Whole-mount microscopy. The collected tissues at the indicated time points were washed in PBS (pH 7.4) twice and set down gently on an agar gel in a petri dish. The whole-mount bright-field and fluorescence images were taken using the Zeiss stereo microscope (AxioZoom V16), and automated *z*-stack images were acquired to determine magnification of the boxed regions.

Immunofluorescence staining. Immunofluorescence staining was performed as previously described[51]. Briefly, tissues were collected in PBS, fixed in 4% paraformaldehyde for 0.5–1 h at 4 °C, washed in PBS three times at room temperature and dehydrated in 30% sucrose overnight at 4 °C. The tissues were then embedded in optimum cutting tissue for 1 h at 4 °C, and frozen in block with optimum cutting tissue and sectioned (Thermo HM525 cryosection machine) or stored at −80 °C. Cryosections at a thickness of 10 µm were collected on slides, washed in PBS, incubated in 5% normal donkey serum in PBST (PBS with 0.1% Triton X-100) for 0.5 h at room temperature and incubated with primary antibodies diluted in 2.5% normal donkey serum in PBST overnight at 4 °C. All primary antibodies were commercially available reagents as follows (including dilutions): ZsGreen (Clontech, 632474; 1:1,000), insulin (Dako, A0564; 1:500), glucagon (Sigma, SAB4501137; 1:500), somatostatin (Santa Cruz, sc-47707; 1:500), somatostatin (Abcam, ab-111912; 1:500), pancreatic polypeptide (Abcam, ab77192; 1:500), pancreatic polypeptide (Abcam, ab255827; 1:500), E-cadherin (Cell Signaling, 3195; 1:500), amylase (Sigma, A8273; 1:500), cytokeratin 19 (Developmental Studies Hybridoma Bank, TROMA-III; 1:200), PDGFRa (R&D, AF1062; 1:500), VE-cadherin (R&D, AF1002; 1:100), lymphatic vessel endothelial hyaluronan receptor 1 (Abcam, ab14917; 1:500), EdU (Invitrogen, C10338; 1:400), DTR (R&D, AF-259-NA; 1:200), GLUT2 (Abcam, ab54460; 1:500), Nkx6.1 (Abcam, ab221549; 1:500) and Pdx1 (Abcam, ab47267; 1:500). After washing, signals were developed with the secondary Alexa Fluor-conjugated antibodies (Invitrogen, 1:1,000) for 0.5 h at room temperature, and cell nuclei were counterstained with DAPI. After, slides were rinsed with PBS and mounted with fluorescence-protecting mounting medium (Vector Labs). Images were obtained with a confocal microscopy system (Nikon A1), and imaging data were analysed using the National Institutes of Health ImageJ software.

H&E staining. H&E staining was performed as previously described[52]. Briefly, 10-µm-thick cryosections were incubated in haematoxylin A solution for 3 mins, washed with tap water three times, rinsed in 1% concentrated hydrochloric acid diluted in 70% ethanol for 1 min and washed with water three times. The slides were then incubated in a 1% ammonia water solution for 1 min, washed three times, stained with eosin Y solution for 8–10 s, dehydrated in a series of ethanol and xylene, and lastly, mounted with neural balsam. All imaging data were acquired using an Olympus microscope (DP72).

Statistical analysis. All mice were randomly assigned to different groups, and all data were obtained from five individual samples, as indicated in each experiment. For all experimental data, calculations were performed in Prism (GraphPad). Unpaired, two-tailed Student's *t*-tests were performed to analyse the *P* value for single comparisons between two groups. Significance was accepted when $P < 0.05$. All data are presented as the mean ± s.e.m. All experiments were performed blinded, and no predetermination was done for sample size.

Reporting Summary. Further information on research design is available in the Nature Research Reporting Summary linked to this article.

Data availability

Newly generated mouse lines will be deposited in a commercial animal repository and will be available, together with data that support the plots and findings within this paper, from the corresponding author upon reasonable request. Source data are provided with this paper.

Received: 3 October 2020; Accepted: 16 February 2021;
Published online: 15 March 2021

References

1. McCarthy, M. I. Genomics, type 2 diabetes and obesity. *N. Engl. J. Med.* **363**, 2339–2350 (2010).
2. Butler, A. E. et al. Beta-cell deficit and increased beta-cell apoptosis in humans with type 2 diabetes. *Diabetes* **52**, 102–110 (2003).
3. Zhou, Q. & Melton, D. A. Pancreas regeneration. *Nature* **557**, 351–358 (2018).
4. Aguayo-Mazzucato, C. & Bonner-Weir, S. Pancreatic beta-cell regeneration as a possible therapy for diabetes. *Cell Metab.* **27**, 57–67 (2018).
5. Dor, Y., Brown, J., Martinez, O. I. & Melton, D. A. Adult pancreatic beta cells are formed by self-duplication rather than stem cell differentiation. *Nature* **429**, 41–46 (2004).
6. Georgia, S. & Bhushan, A. Beta-cell replication is the primary mechanism for maintaining postnatal beta cell mass. *J. Clin. Invest.* **114**, 963–968 (2004).
7. Teta, M., Rankin, M. M., Long, S. Y., Stein, G. M. & Kushner, J. A. Growth and regeneration of adult beta cells does not involve specialized progenitors. *Dev. Cell* **12**, 817–826 (2007).
8. Nir, T., Melton, D. A. & Dor, Y. Recovery from diabetes in mice by beta-cell regeneration. *J. Clin. Invest.* **117**, 2553–2561 (2007).
9. Hao, E. et al. Beta-cell differentiation from nonendocrine epithelial cells of the adult human pancreas. *Nat. Med.* **12**, 310–316 (2006).
10. Thorel, F. et al. Conversion of adult pancreatic alpha cells to beta cells after extreme beta-cell loss. *Nature* **464**, 1149–1154 (2010).
11. Chera, S. et al. Diabetes recovery by age-dependent conversion of pancreatic delta cells into insulin producers. *Nature* **514**, 503–507 (2014).
12. Al-Hasani, K. et al. Adult duct-lining cells can reprogram into beta-like cells able to counter repeated cycles of toxin-induced diabetes. *Dev. Cell* **26**, 86–100 (2013).
13. Courtney, M. et al. The inactivation of Arx in pancreatic alpha cells triggers their neogenesis and conversion into functional beta-like cells. *PLoS Genet.* **9**, e1003934 (2013).
14. Furuyama, K. et al. Diabetes relief in mice by glucose-sensing insulin-secreting human alpha cells. *Nature* **567**, 43–48 (2019).
15. Zhou, Q., Brown, J., Kanarek, A., Rajagopal, J. & Melton, D. A. In vivo reprogramming of adult pancreatic exocrine cells to beta cells. *Nature* **455**, 627–632 (2008).
16. Miyazaki, S., Tashiro, F. & Miyazaki, J. Transgenic expression of a single transcription factor Pdx1 induces transdifferentiation of pancreatic acinar cells to endocrine cells in adult mice. *PLoS ONE* **11**, e0161190 (2016).
17. Xu, X. et al. Beta cells can be generated from endogenous progenitors in injured adult mouse pancreas. *Cell* **132**, 197–207 (2008).
18. Inada, A. et al. Carbonic anhydrase II-positive pancreatic cells are progenitors for both endocrine and exocrine pancreas after birth. *Proc. Natl Acad. Sci. USA* **105**, 19915–19919 (2008).
19. Pan, F. C. et al. Spatiotemporal patterns of multipotentiality in Ptf1a-expressing cells during pancreas organogenesis and injury-induced facultative restoration. *Development* **140**, 751–764 (2013).
20. Jin, L. et al. Cells with surface expression of $CD133^{high}CD71^{low}$ are enriched for tripotent colony-forming progenitor cells in the adult murine pancreas. *Stem Cell Res.* **16**, 40–53 (2016).
21. Rovira, M. et al. Isolation and characterization of centroacinar/terminal ductal progenitor cells in adult mouse pancreas. *Proc. Natl Acad. Sci. USA* **107**, 75–80 (2010).
22. Criscimanna, A. et al. Duct cells contribute to regeneration of endocrine and acinar cells following pancreatic damage in adult mice. *Gastroenterology* **141**, 1451–1462 (2011).
23. El-Gohary, Y. et al. Intraislet pancreatic ducts can give rise to insulin-positive cells. *Endocrinology* **157**, 166–175 (2016).
24. Wang, D. et al. Long-term expansion of pancreatic islet organoids from resident $Procr^{+}$ progenitors. *Cell* **180**, 1198–1211 (2020).
25. Solar, M. et al. Pancreatic exocrine duct cells give rise to insulin-producing beta cells during embryogenesis but not after birth. *Dev. Cell* **17**, 849–860 (2009).
26. Kopinke, D. & Murtaugh, L. C. Exocrine-to-endocrine differentiation is detectable only prior to birth in the uninjured mouse pancreas. *BMC Dev. Biol.* **10**, 38 (2010).
27. Kopp, J. L. et al. $Sox9^{+}$ ductal cells are multipotent progenitors throughout development but do not produce new endocrine cells in the normal or injured adult pancreas. *Development* **138**, 653–665 (2011).
28. Kopinke, D. et al. Lineage tracing reveals the dynamic contribution of $Hes1^{+}$ cells to the developing and adult pancreas. *Development* **138**, 431–441 (2011).
29. Xiao, X. et al. No evidence for beta-cell neogenesis in murine adult pancreas. *J. Clin. Invest.* **123**, 2207–2217 (2013).
30. Sauer, B. & McDermott, J. DNA recombination with a heterospecific Cre homolog identified from comparison of the *pac-c1* regions of P1-related phages. *Nucleic Acids Res.* **32**, 6086–6095 (2004).
31. Anastassiadis, K. et al. Dre recombinase, like Cre, is a highly efficient site-specific recombinase in *E. coli*, mammalian cells and mice. *Dis. Model. Mech.* **2**, 508–515 (2009).

32. Hermann, M. et al. Binary recombinase systems for high-resolution conditional mutagenesis. *Nucleic Acids Res.* **42**, 3894–3907 (2014).
33. He, L. et al. Enhancing the precision of genetic lineage tracing using dual recombinases. *Nat. Med.* **23**, 1488–1498 (2017).
34. Zhou, Q. et al. A multipotent progenitor domain guides pancreatic organogenesis. *Dev. Cell* **13**, 103–114 (2007).
35. Xiao, X. et al. TGFβ receptor signaling is essential for inflammation-induced but not beta-cell workload-induced beta-cell proliferation. *Diabetes* **62**, 1217–1226 (2013).
36. Rankin, M. M. et al. Beta cells are not generated in pancreatic duct ligation-induced injury in adult mice. *Diabetes* **62**, 1634–1645 (2013).
37. Talchai, C., Xuan, S., Lin, H. V., Sussel, L. & Accili, D. Pancreatic beta-cell dedifferentiation as a mechanism of diabetic beta-cell failure. *Cell* **150**, 1223–1234 (2012).
38. Rahier, J., Guiot, Y., Goebbels, R. M., Sempoux, C. & Henquin, J. C. Pancreatic beta-cell mass in European subjects with type 2 diabetes. *Diabetes Obes. Metab.* **10**, 32–42 (2008).
39. Butler, A. E. et al. Beta-cell deficit in obese type 2 diabetes, a minor role of beta-cell dedifferentiation and degranulation. *J. Clin. Endocrinol. Metab.* **101**, 523–532 (2016).
40. Kim, H. et al. Serotonin regulates pancreatic beta-cell mass during pregnancy. *Nat. Med.* **16**, 804–808 (2010).
41. Wuidart, A. et al. Quantitative lineage tracing strategies to resolve multipotency in tissue-specific stem cells. *Genes Dev.* **30**, 1261–1277 (2016).
42. Ma, Q., Zhou, B. & Pu, W. T. Reassessment of *Isl1* and *Nkx2-5* cardiac fate maps using a *Gata4*-based reporter of Cre activity. *Dev. Biol.* **323**, 98–104 (2008).
43. Tasic, B. et al. Site-specific integrase-mediated transgenesis in mice via pronuclear injection. *Proc. Natl Acad. Sci. USA* **108**, 7902–7907 (2011).
44. Tian, X., Pu, W. T. & Zhou, B. Cellular origin and developmental program of coronary angiogenesis. *Circ. Res.* **116**, 515–530 (2015).
45. Zhao, H. & Zhou, B. Dual genetic approaches for deciphering cell fate plasticity in vivo: more than double. *Curr. Opin. Cell Biol.* **61**, 101–109 (2019).
46. Hochedlinger, K., Yamada, Y., Beard, C. & Jaenisch, R. Ectopic expression of *Oct-4* blocks progenitor-cell differentiation and causes dysplasia in epithelial tissues. *Cell* **121**, 465–477 (2005).
47. Perl, A. K., Wert, S. E., Nagy, A., Lobe, C. G. & Whitsett, J. A. Early restriction of peripheral and proximal cell lineages during formation of the lung. *Proc. Natl Acad. Sci. USA* **99**, 10482–10487 (2002).
48. Li, Y. et al. Genetic lineage tracing of non-myocyte population by dual recombinases. *Circulation* **138**, 793–805 (2018).
49. Madisen, L. et al. A robust and high-throughput Cre reporting and characterization system for the whole mouse brain. *Nat. Neurosci.* **13**, 133–140 (2010).
50. Zhang, H. et al. Endocardium minimally contributes to coronary endothelium in the embryonic ventricular free walls. *Circ. Res.* **118**, 1880–1893 (2016).
51. Tian, X. et al. De novo formation of a distinct coronary vascular population in neonatal heart. *Science* **345**, 90–94 (2014).
52. Zhao, H. et al. Apj$^+$ vessels drive tumor growth and represent a tractable therapeutic target. *Cell Rep.* **25**, 1241–1254 2018).

Acknowledgements

We thank Shanghai Biomodel Organism for mouse generation and H. Zeng for reporter mice. This study was supported by the National key Research & Development Program of China (2019YFA0802000, 2019YFA0110403, 2018YFA0108100, 2017YFC1001303, 2020YFA0803202, 2019YFA0802803 and 2018YFA0107900), Strategic Priority Research Program of the Chinese Academy of Sciences (CAS; XDB19000000 and XDA16010507), National Science Foundation of China (31730112, 82088101, 32050087, 91849202, 31625019, 31922032, 81872241 and 31900625), Key Project of Frontier Sciences of CAS (QYZDB-SSW-SMC003), Shanghai Science and Technology Commission (19JC1415700, 20QC1401000, 19YF1455300 and 19ZR1479800), Collaborative Innovation Program of Shanghai Municipal Health Commission (2020CXJQ01), China Postdoctoral Science Foundation, National Postdoctoral Program for Innovative Talents (BX20190343, 2019M660100, 2020TQ0336 and 2020M681409), the Pearl River Talent Recruitment Program of Guangdong Province (2017ZT07S347), Royal Society-Newton Advanced Fellowship, AstraZeneca, Boehringer-Ingelheim, Sanofi-SIBS Fellowship, SIBS President Fund and the support from the Xplorer Prize.

Author contributions

H.Z. and B.Z. designed the study, performed experiments and analysed the data. X.H., Z. Liu, W.P., L.H. and Z. Lv bred the mice, performed experiments or provided valuable comments. Q.Z. provided valuable comments and suggestions, and edited the manuscript. Y.L. and K.O.L. contributed to interpreting the data and writing the manuscript. B.Z. supervised the study, analysed the data and wrote the manuscript.

Competing interests

The authors declare no competing interests.

Additional information

Extended data is available for this paper at https://doi.org/10.1038/s42255-021-00364-0.

Supplementary information The online version contains supplementary material available at https://doi.org/10.1038/s42255-021-00364-0.

Correspondence and requests for materials should be addressed to B.Z.

Peer review information *Nature Metabolism* thanks the anonymous reviewers for their contribution to the peer review of this work. Primary Handling Editor: Christoph Schmitt.

Reprints and permissions information is available at www.nature.com/reprints.

Publisher's note Springer Nature remains neutral with regard to jurisdictional claims in published maps and institutional affiliations.

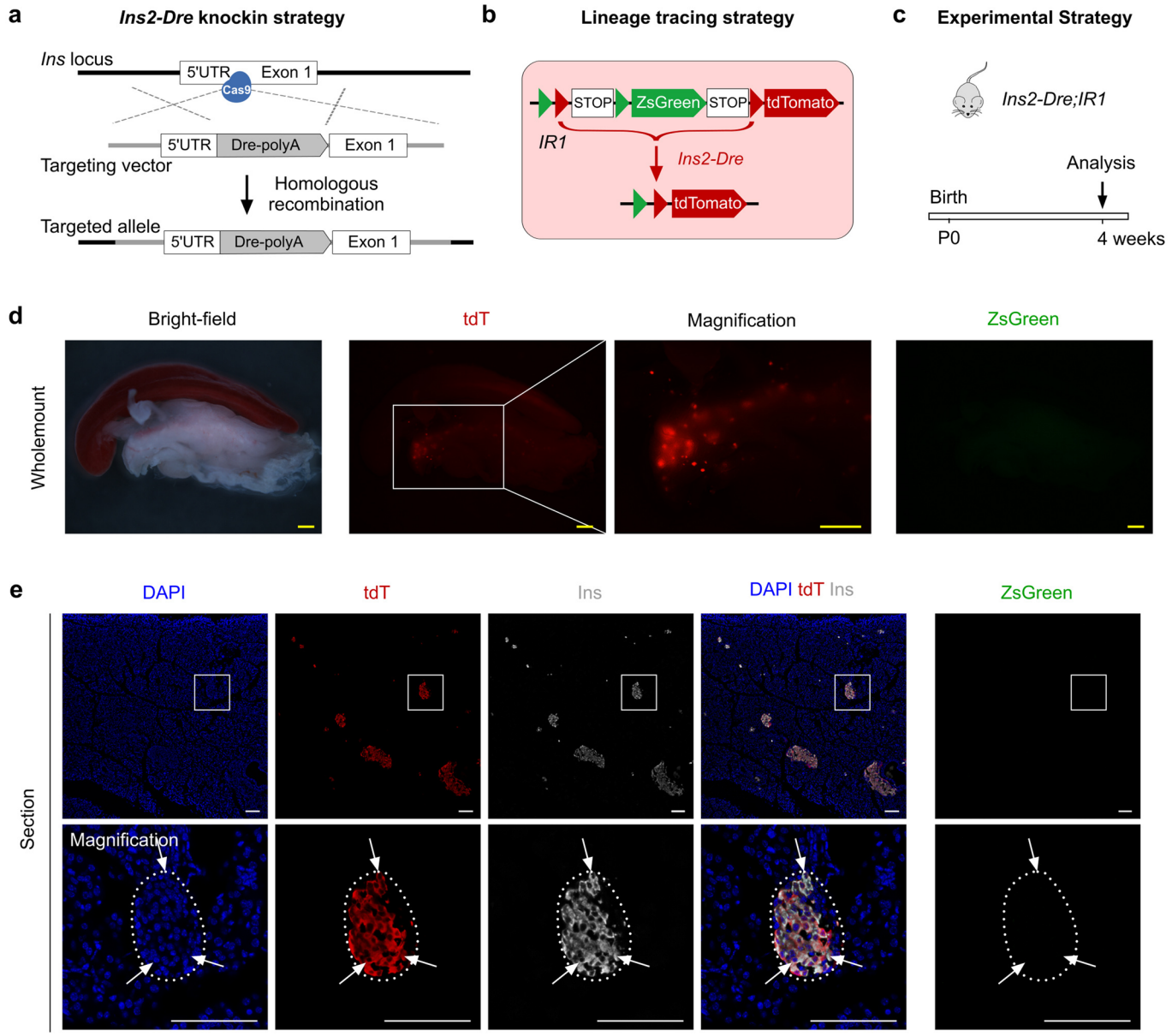

Extended Data Fig. 1 | Generation and characterization of *Ins2-Dre* mouse allele. a, A Schematic diagram illustrating knock-in strategy for *Ins2-Dre* by homologous recombination using CRISPR/Cas9. **b**, A Schematic diagram illustrating the strategy for labeling pancreatic β cells by *Ins2-Dre* using interleaved reporter 1 (*IR1*). **c**, A Schematic diagram illustrating the experimental strategy. 4 weeks old mice (both male and female mice were used) were euthanized for analysis (n = 5). **d**, Whole-mount bright-field and fluorescent images of pancreas from *Ins2-Dre;IR1*. **e**, Immunostaining for tdT, zsGreen, and Ins on pancreatic slides collected from *Ins2-Dre;IR1*. Arrows indicate $tdT^{+}Ins^{+}$ β cells. Scale bars, yellow, 1 mm; white, 100 μm. Each image is representative of 5 individual biological samples.

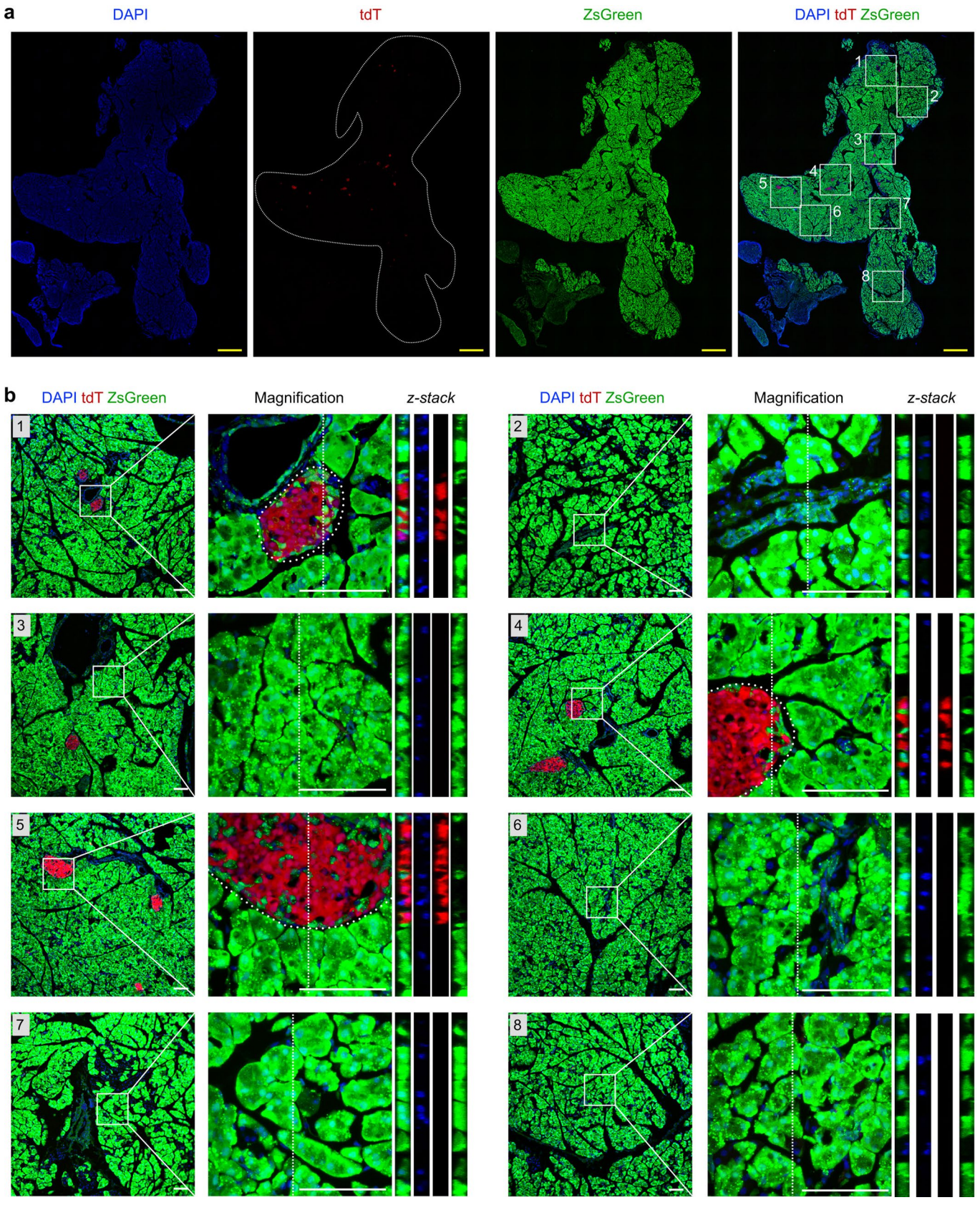

Extended Data Fig. 2 | *Ins2-Dre;R26-iCre;IR1* efficiently labels most of cells in pancreas. (**a-b**) Immunostaining for tdT and zsGreen on slides collected from *Ins2-Dre;R26-iCre;IR1* mice at 7 weeks old after Dox treatment (both male and female mice were used, n = 5). Boxed regions in (**a**) are magnified in (**b**). Scale bars, yellow, 1mm; white, 100 μm. Each image is representative of 5 individual biological samples.

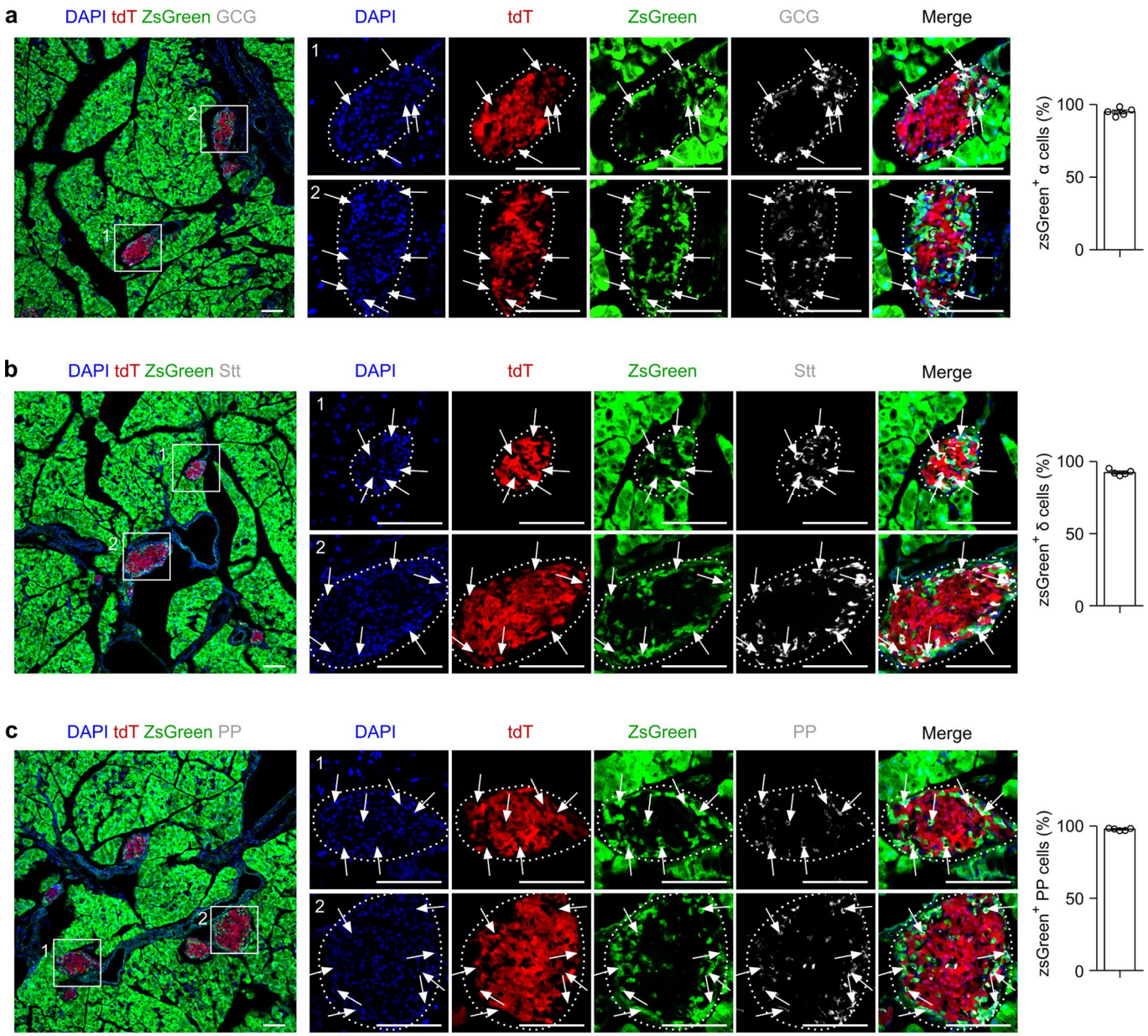

Extended Data Fig. 3 | *R26-iCre* efficiently labels most of cell lineages in pancreatic endocrine glands. (**a-c**) Immunostaining for tdT, zsGreen, Glucagon (GCG, a), Somatostatin (Stt, b) and Pancreatic Polypeptide (PP, c) on slides collected from *Ins2-Dre;R26-iCre;IR1* mice at 7 weeks old after Dox treatment (both male and female mice were used, n = 5). Arrows indicate zsGreen$^+$ cell lineages. Right panel is the quantification of the percentage of indicated non-β cell lineages expressing zsGreen. Data are mean ± SEM, n = 5. Scale bars, 100 μm. Each image is representative of 5 individual biological samples.

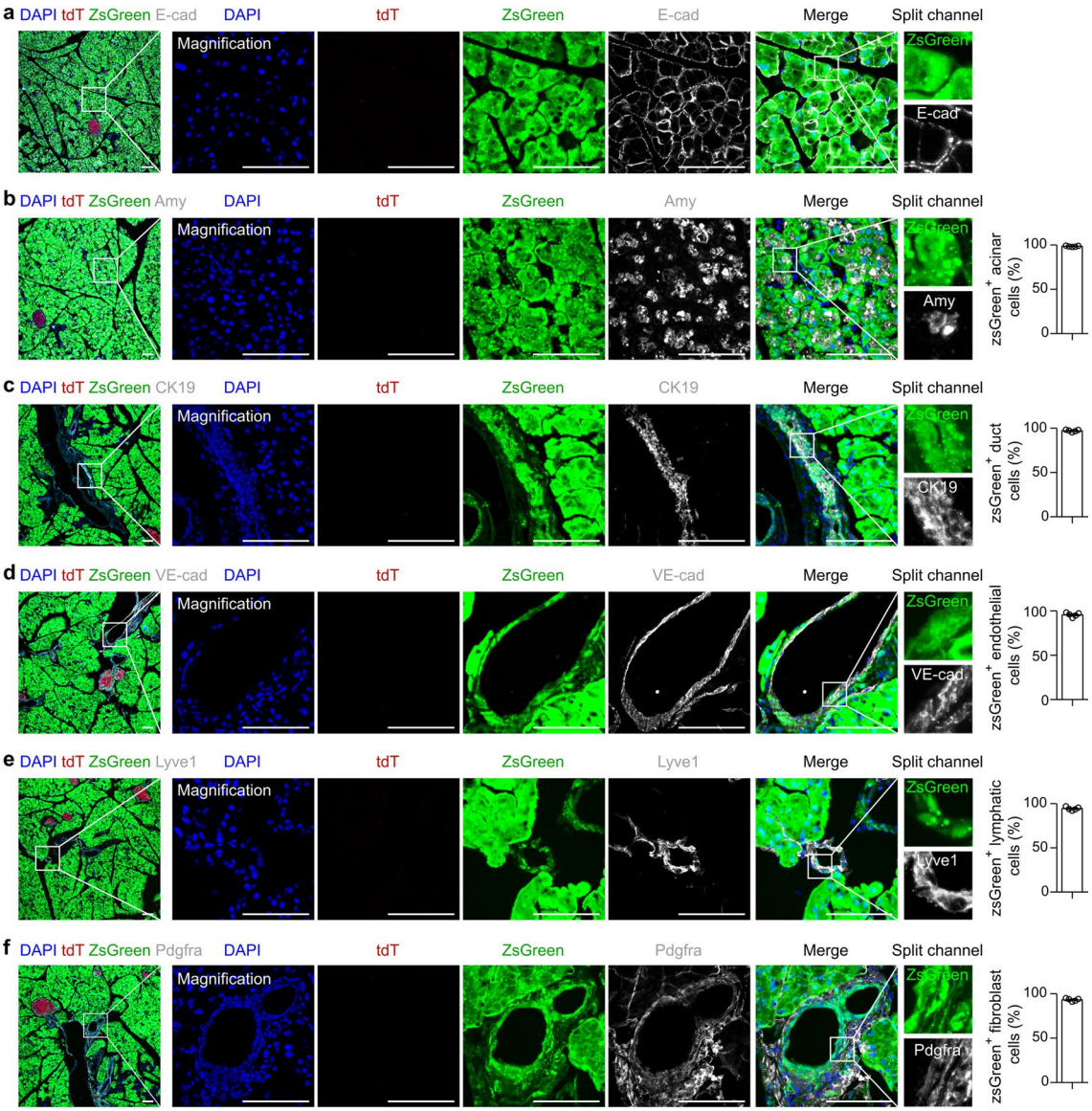

Extended Data Fig. 4 | *R26-iCre* efficiently labels most of cell lineages in pancreatic exocrine gland. (**a-f**) Immunostaining for tdT, zsGreen and E-cadherin (E-cad), or Amylase (Amy), Cytokeratin 19 (CK19), Vascular endothelial cadherin (VE-cad), Lymphatic vessel endothelial hyaluronan receptor 1 (Lyve1) and Platelet derived growth factor receptor a (Pdgfra) on slides collected from *Ins2-Dre;R26-iCre;IR1* mice at 7 weeks old after Dox treatment (both male and female mice were used, n = 5). Right panel is the quantification of the percentage of indicated non-β cell lineages expressing zsGreen. Data are mean ± SEM, n = 5 (Dox group). Scale bars, 100 μm. Each image is representative of 5 individual biological samples.

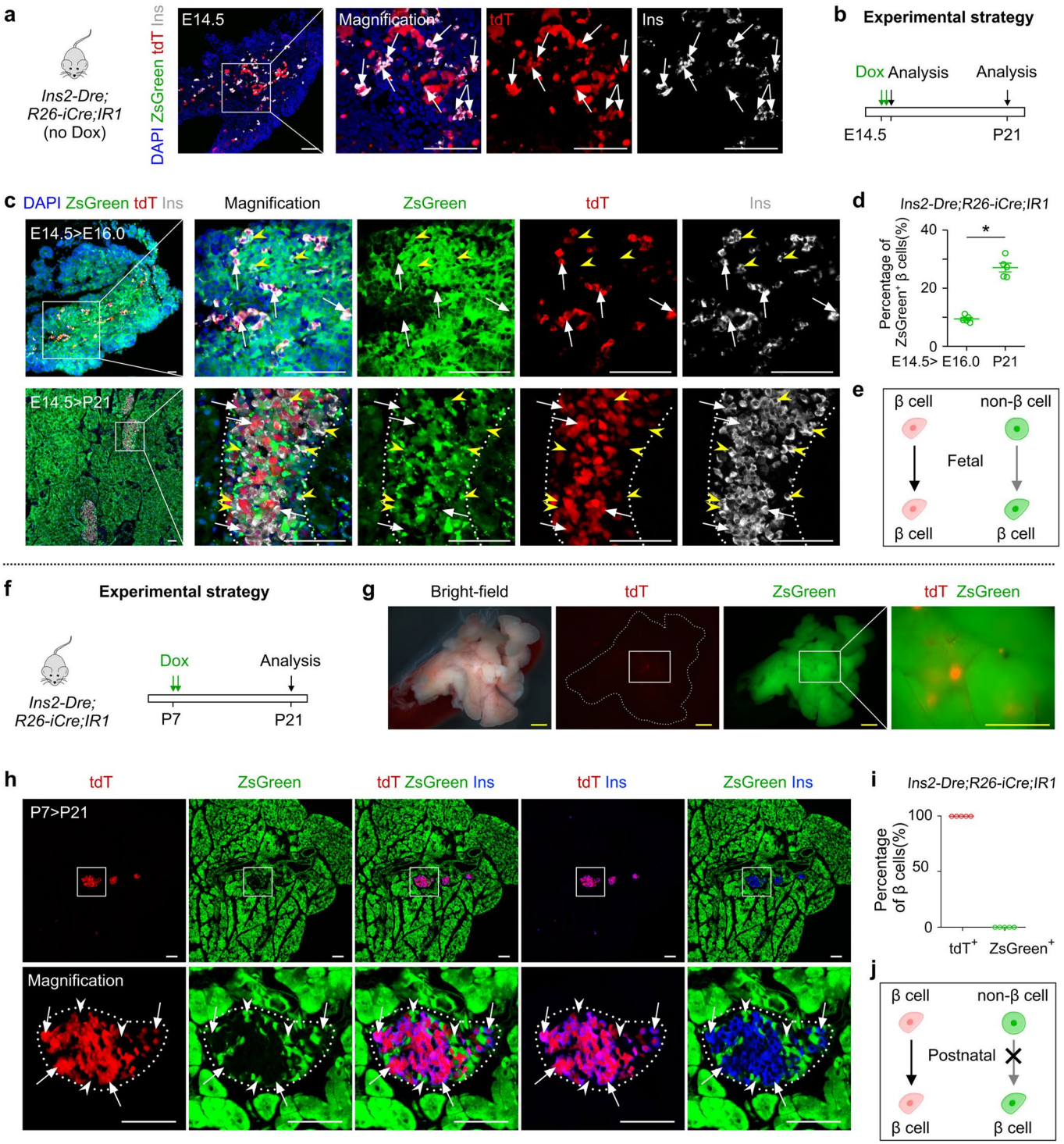

Extended Data Fig. 5 | Non-β cells contribute to β cells in embryonic stage. a, Immunostaining for tdT, zsGreen, and Ins on pancreatic sections of *Ins-Dre;R26-iCre;IR1* mice without Dox treatment at E14.5 (both male and female mice were used, n = 5). **b**, A schematic figure showing experimental strategy of Dox injection and analysis. **c**, Immunostaining for tdT, zsGreen, and Ins on pancreatic sections of *Ins-Dre;R26-iCre;IR1* mice at E16.0 (top) and P21 (bottom) treated with Dox at E14.5 (both male and female mice were used, E16.0 group, n = 5; P21 group, n = 5). White arrows indicate tdT$^+$Ins$^+$ β cells. Yellow arrowheads indicate zsGreen$^+$Ins$^+$ β cells. **d**, Quantification of the percentage of zsGreen$^+$ β cells from indicated mice. Numbers of investigated mice were as follows: E14.5>E16.0 group, n = 5; E14.5>P21 group, n = 5, Data are mean ± SEM, P=1.12×10^{-4}, *P<0.05 (unpaired, two-sided, Student's t-test). **e**, Illustration showing contribution of non-β cells to β cells in embryonic stage. **f**, A schematic figure showing experimental strategy of Dox injection and analysis (both male and female mice were used, n = 5). **g**, Whole-mount bright-field and fluorescent images of pancreas from *Ins-Dre;R26-iCre;IR1* mice with Dox treatment. **h**, Immunostaining for tdT, zsGreen, and Ins on pancreatic sections of *Ins-Dre;R26-iCre;IR1* mice at P21 with Dox treatment at P7. Arrows indicate tdT$^+$Ins$^+$ β cells. Arrowheads indicate zsGreen$^+$Ins$^-$ non-β cells. **i**, Quantification of the percentage of β cells expressing tdT or zsGreen from indicated mice. Data are mean ± SEM, n=5 (P7>P21 group). (**j**) Illustration showing no contribution of non-β cells to β cells in postnatal stage. Scale bars, yellow, 1 mm; white, 100 μm. Each image is representative of 5 individual samples.

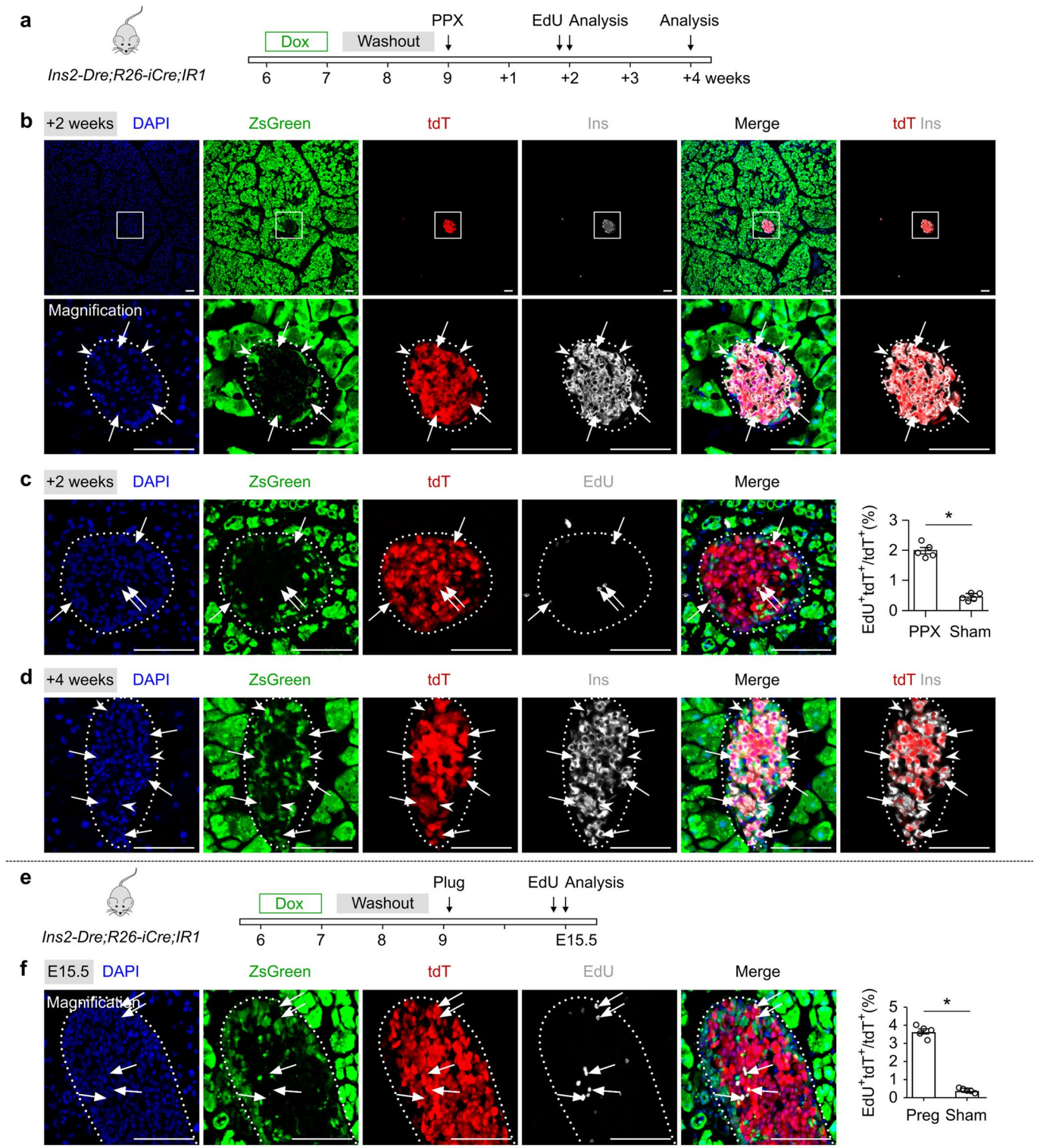

Extended Data Fig. 6 | See next page for caption.

Extended Data Fig. 6 | β cells proliferate after partial pancreatectomy and during pregnancy. a, A schematic diagram illustrating the experimental strategy for Dox induction, partial pancreatectomy (PPX) and analysis. 6 weeks old mice (both male and female mice were used) were treated with Dox for 1 week. After washout for 2 weeks and PPX injury for 2 and 4 weeks, mice were euthanized (PPX group: n = 5; Sham group: n = 5). **b**, Immunostaining for tdT, ZsGreen and Ins on pancreatic sections collected after PPX 2 weeks. Arrows indicate tdT^+Ins^+ β cells. Arrowheads indicate $zsGreen^+Ins^-$ non-β cells. **c**, Immunostaining on pancreatic sections for tdT, ZsGreen and EdU collected after PPX 2 weeks. Arrows indicate EdU^+tdT^+ cells. EdU was injected 12 hours before sacrifice. Right panel shows quantification of the percentage of tdT+ cells with incorporated EdU. Numbers of investigated mice were as follows: PPX group, n = 5; Sham group, n = 5, Data are mean ± SEM, $P=1.22\times10^{-5}$, $^*P<0.05$ (unpaired, two-sided, Student's *t*-test). **d**, Immunostaining for tdT, ZsGreen and Ins on pancreatic sections collected after PPX 4 weeks. Arrows indicate tdT^+Ins^+ β cells. Arrowheads indicate $zsGreen^+Ins^-$ non-β cells. **e**, A schematic diagram illustrating experimental strategy of Dox induction, pregnancy and analysis. 6 weeks old mice (only female mice were used) were treated with Dox for 1 week. After washout for 2 weeks and Pregnancy for 15.5 d, mice were euthanized (Pregnancy group: n = 5; Sham group: n = 5). **f**, Immunostaining for tdT, ZsGreen and EdU on pancreatic sections collected after pregnancy. Arrows indicate EdU^+tdT^+ cells. EdU was injected 12 hours before sacrifice. Right panel shows quantification of the percentage of tdT^+ cells with incorporated EdU. Numbers of investigated mice were as follows: Pregnancy group, n = 5; Sham group, n = 5, Data are mean ± SEM, $P=3.38\times10^{-6}$, $^*P<0.05$ (unpaired, two-sided, Student's *t*-test). Scale bars, 100 μm. Each image is representative of 5 individual samples.

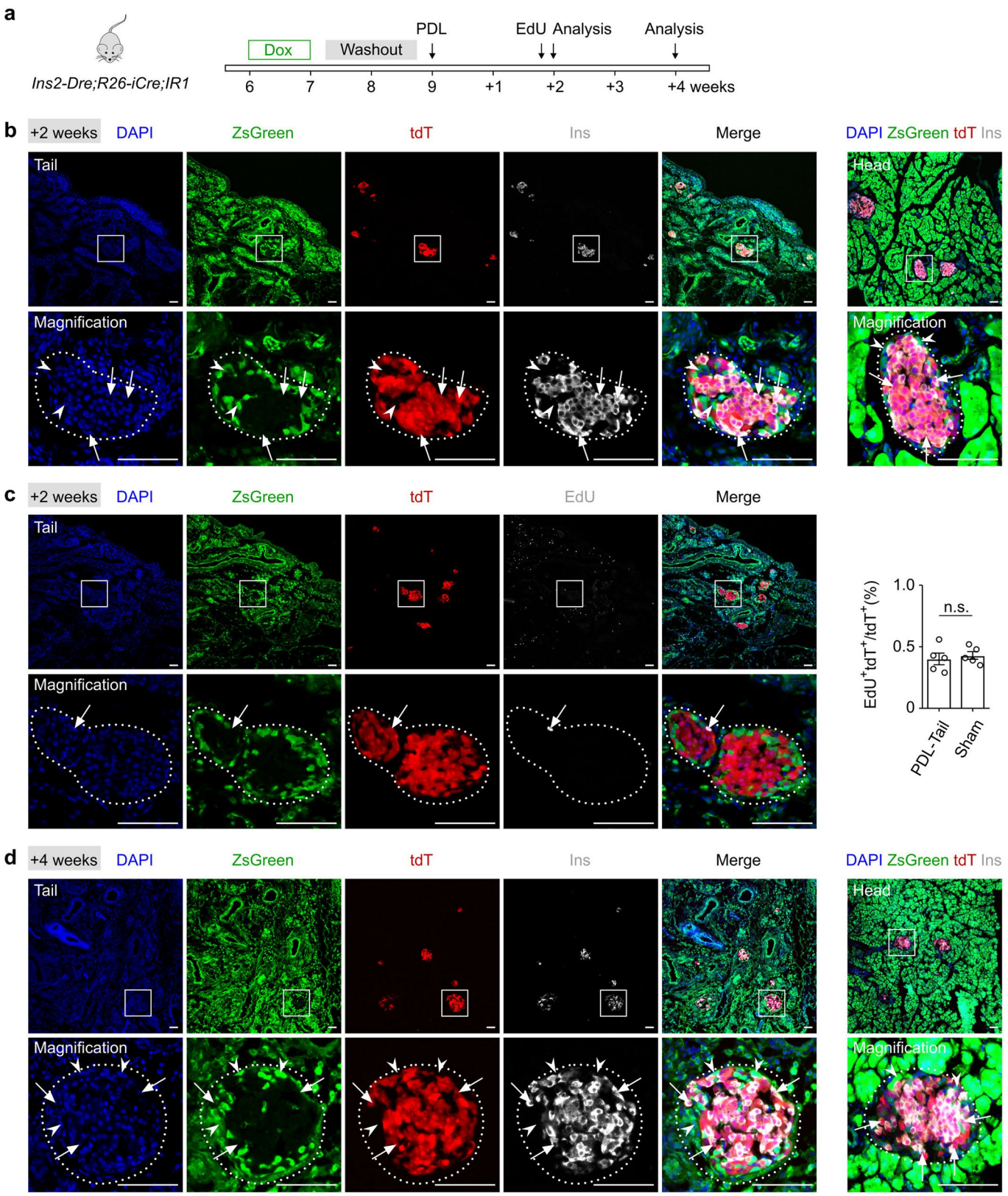

Extended Data Fig. 7 | See next page for caption.

Extended Data Fig. 7 | β cells are not generated from non-β cells after pancreatic ductal ligation. a, A schematic diagram illustrating experimental strategy of Dox induction, pancreatic ductal ligation (PDL) and analysis. 6 weeks old mice (both male and female mice were used) were treated with Dox for 1 week. After washout for 2 weeks and PDL injury for 2 and 4 weeks, mice were euthanized (PDL group: n = 5; Sham group: n = 5). **b**, Immunostaining for tdT, ZsGreen and Ins on pancreatic tail (left) and head (right) sections collected after PDL 2 weeks. Arrows indicate tdT^+Ins^+ β cells. Arrowheads indicate $zsGreen^+Ins^-$ non-β cells. **c**, Immunostaining for tdT, ZsGreen and EdU collected after PDL. Arrowheads indicate EdU^+tdT^+ cells. EdU was injected 12 hours before sacrifice. Right panel shows quantification of the percentage of tdT+ cells with incorporated EdU. Numbers of investigated mice were as follows: PDL group, n = 5; Sham group, n = 5, Data are mean ± SEM, n.s., not significant (unpaired, two-sided, Student's *t*-test). **d**, Immunostaining for tdT, ZsGreen and Ins on pancreatic tail (left) and head (right) sections collected after PDL 4 weeks. Arrows indicate tdT^+Ins^+ β cells. Arrowheads indicate $zsGreen^+Ins^-$ non-β cells. Scale bars, 100 μm. Each image is representative of 5 individual samples.

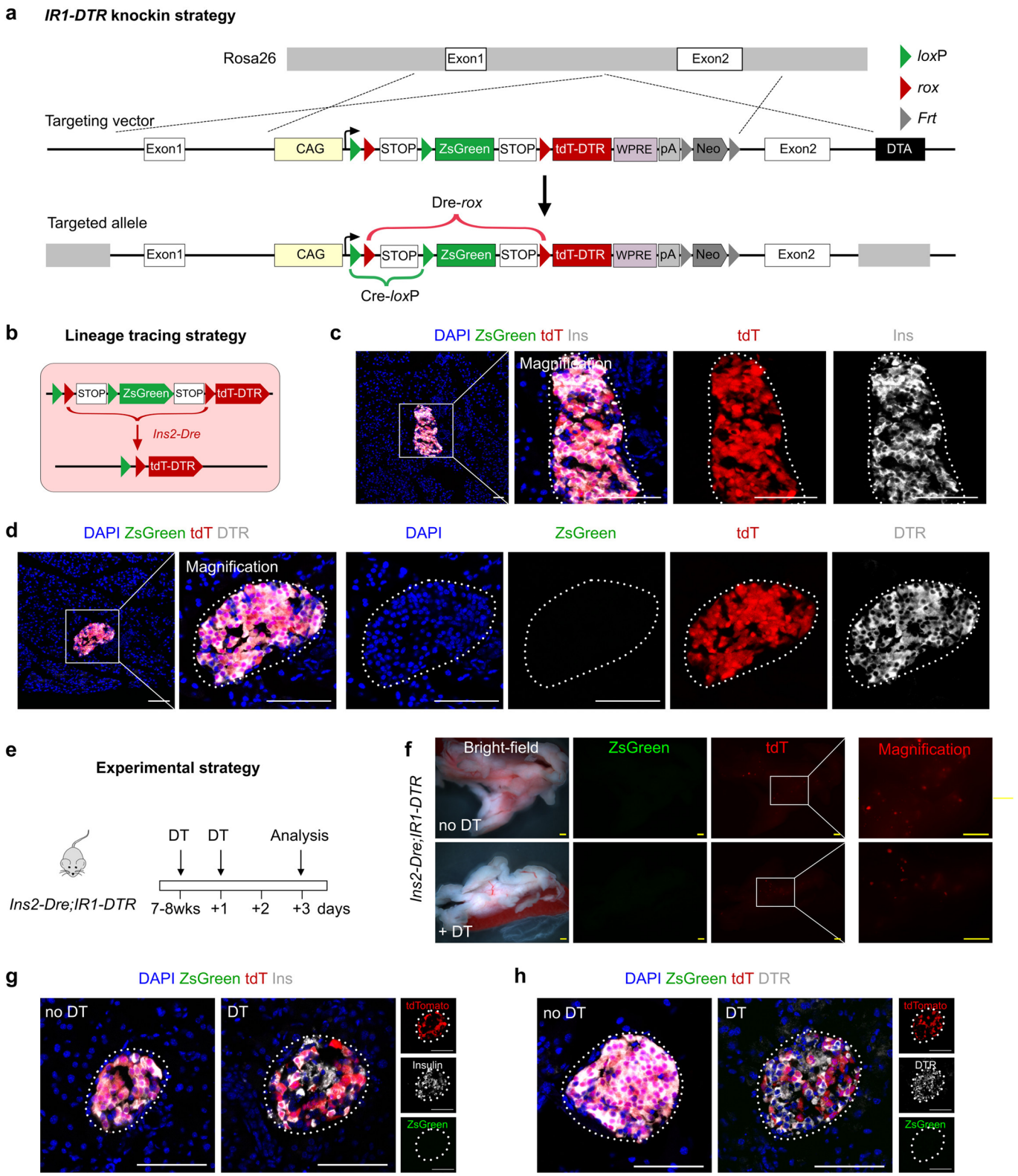

Extended Data Fig. 8 | Generation and characterization of *IR1-DTR*. **a**, A schematic diagram illustrating knock-in strategy for generation of *IR1-DTR* by homologous recombination using CRISPR/Cas9. **b**, Strategy for labeling pancreatic β cells by *Ins2-Dre;IR1-DTR* mouse line. **c**, Immunostaining for tdT, zsGreen and Ins on pancreatic slides collected from 8 weeks old *Ins2-Dre;IR1-DTR* (both male and female mice were used, n = 5). **d**, Immunostaining for tdT, zsGreen, and DTR on pancreatic slides collected from 8 weeks old *Ins2-Dre;IR1-DTR*. **e**, A schematic figure showing experimental strategy of DT injection and analysis. 7–8 weeks old mice (both male and female mice were used) were treated with DT for 2 times. After 3 days, mice were euthanized (DT group: n = 5; no DT group: n = 5). **f**, Whole-mount bright-field and fluorescent images of pancreas from *Ins2-Dre;IR1-DTR* mice. **g**, Immunostaining for tdT, zsGreen, and Ins on pancreatic sections of *Ins2-Dre;IR1-DTR* mice. **h**, Immunostaining for tdT, zsGreen, and DTR on pancreatic sections of *Ins2-Dre;IR1-DTR* mice. Scale bars, yellow, 1 mm; white, 100 μm. Each image is representative of 5 individual biological samples.

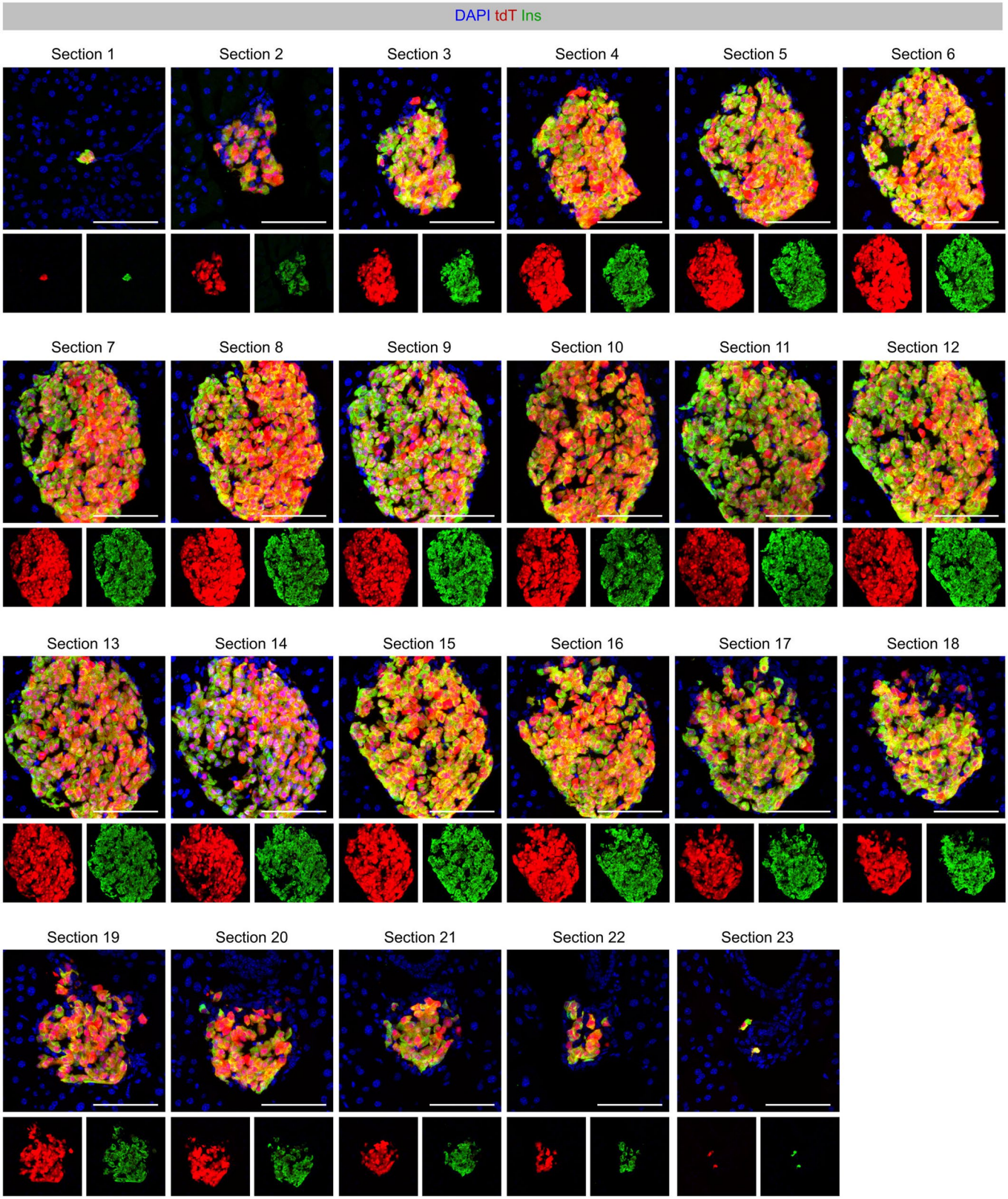

Extended Data Fig. 9 | *Ins2-DreER* specifically and efficiently labels β cells in the adult pancreas. Immunostaining for tdT and Insulin on consecutive sections (section 1–23) of pancreatic islets of 8 weeks old *Ins2-DreER;H11-rox-tdT* mice treated with Tam (both male and female mice were used, n = 5). Scale bars, 100 μm. This data is representative of 5 individual biological samples.

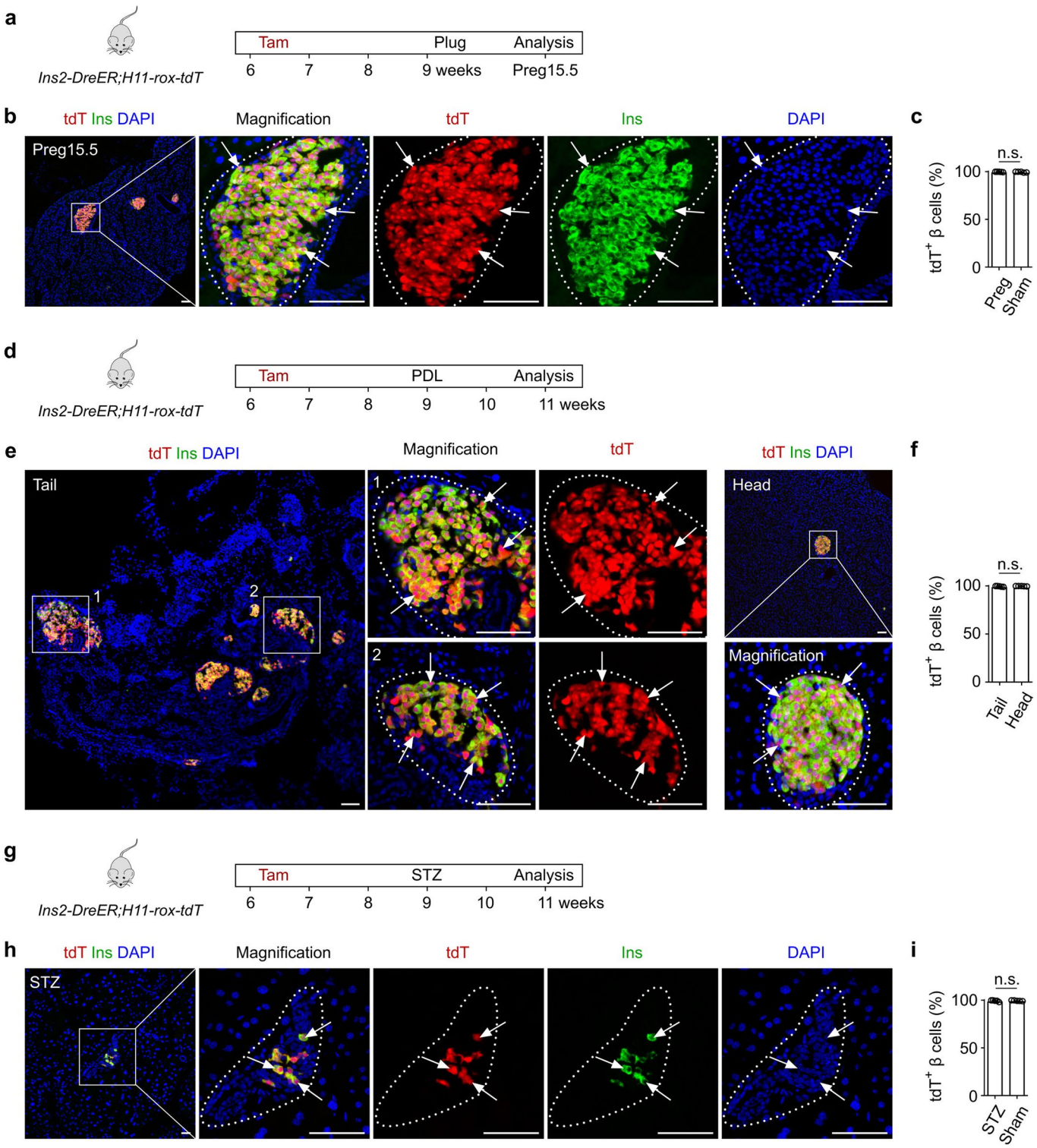

Extended Data Fig. 10 | See next page for caption.

Extended Data Fig. 10 | Analysis of β cells after injuries by inducible *Ins2-DreER;H11-rox-tdT* system. a, A schematic diagram illustrating the experimental design to test for β cell neogenesis during pregnancy in the inducible system. 6 weeks old mice (only female mice were used) were treated with Tamoxifen for 3 times. After washout for 2 weeks and Pregnancy for 15.5 days, mice were euthanized (Pregnancy group, n = 5; Sham group, n = 5). **b**, Immunostaining for tdT and Ins on pancreatic slides collected from *Ins2-DreER;H11-rox-tdT* during pregnancy (Preg15.5). **c**, Quantification of β cells expressing tdT in the indicated mice. Numbers of investigated mice were as follows: Pregnancy group, n = 5; Sham group, n = 5, Data are mean ± SEM, n.s., not significant (unpaired, two-sided, Student's *t*-test). **d**, A schematic diagram illustrating the experimental design to test for β cell neogenesis after pancreatic ductal ligation (PDL). 6 weeks old mice (both male and female mice were used) were treated with Tamoxifen for 3 times. After washout for 2 weeks and PDL injury for 2 weeks, mice were euthanized (PDL group, n = 5; Sham group, n = 5). **e**, Immunostaining for tdT and Ins on pancreatic slides collected from *Ins2-DreER;H11-rox-tdT* after PDL. **f**, Quantification of β cells expressing tdT in the indicated mice. Numbers of investigated mice were as follows: PDL group, n = 5; Sham group, n = 5, Data are mean ± SEM, n.s., not significant (unpaired, two-sided, Student's *t*-test). **g**, A schematic diagram illustrating the experimental design to test for β cell neogenesis after streptozocin (STZ)-induced injury. 6 weeks old mice (both male and female mice were used) were treated with Tamoxifen for 3 times. After washout for 2 weeks and STZ injury for 2 weeks, mice were euthanized (STZ group, n = 5; Sham group, n = 5). **h**, Immunostaining for tdT and Ins on pancreatic slides collected from *Ins2-DreER;H11-rox-tdT* after streptozocin (STZ)-induced injury. (**i**) Quantification of β cells expressing tdT in the indicated mice. Numbers of investigated mice were as follows: STZ group, n = 5; Sham group, n = 5, Data are mean ± SEM, n.s., not significant (unpaired, two-sided, Student's *t*-test). Scale bars, yellow, 1 mm; white, 100 μm. Each image is representative of 5 individual biological samples.

nature research

Corresponding author(s): Bin Zhou

Last updated by author(s): Feb 16, 2021

Reporting Summary

Nature Research wishes to improve the reproducibility of the work that we publish. This form provides structure for consistency and transparency in reporting. For further information on Nature Research policies, see our Editorial Policies and the Editorial Policy Checklist.

Statistics

For all statistical analyses, confirm that the following items are present in the figure legend, table legend, main text, or Methods section.

n/a	Confirmed	
☐	☒	The exact sample size (*n*) for each experimental group/condition, given as a discrete number and unit of measurement
☐	☒	A statement on whether measurements were taken from distinct samples or whether the same sample was measured repeatedly
☐	☒	The statistical test(s) used AND whether they are one- or two-sided *Only common tests should be described solely by name; describe more complex techniques in the Methods section.*
☒	☐	A description of all covariates tested
☒	☐	A description of any assumptions or corrections, such as tests of normality and adjustment for multiple comparisons
☐	☒	A full description of the statistical parameters including central tendency (e.g. means) or other basic estimates (e.g. regression coefficient) AND variation (e.g. standard deviation) or associated estimates of uncertainty (e.g. confidence intervals)
☐	☒	For null hypothesis testing, the test statistic (e.g. *F*, *t*, *r*) with confidence intervals, effect sizes, degrees of freedom and *P* value noted *Give P values as exact values whenever suitable.*
☒	☐	For Bayesian analysis, information on the choice of priors and Markov chain Monte Carlo settings
☒	☐	For hierarchical and complex designs, identification of the appropriate level for tests and full reporting of outcomes
☒	☐	Estimates of effect sizes (e.g. Cohen's *d*, Pearson's *r*), indicating how they were calculated

Our web collection on statistics for biologists contains articles on many of the points above.

Software and code

Policy information about availability of computer code

Data collection	Zeiss stereoscope (Axio Zoom. V16) was used for whole-mount bright-field and fluorescent image collection. Nikon A1 confocal was used for immunofluorescent data collection.
Data analysis	Image J (FIJI) and Photoline (18.5.1) were used for immunofluorescence and bright-filed images analysis. GraphPad Prism 8.0 was used for data analysis.

For manuscripts utilizing custom algorithms or software that are central to the research but not yet described in published literature, software must be made available to editors and reviewers. We strongly encourage code deposition in a community repository (e.g. GitHub). See the Nature Research guidelines for submitting code & software for further information.

Data

Policy information about availability of data

All manuscripts must include a data availability statement. This statement should provide the following information, where applicable:

- Accession codes, unique identifiers, or web links for publicly available datasets
- A list of figures that have associated raw data
- A description of any restrictions on data availability

All data will be provided upon request.

Field-specific reporting

Please select the one below that is the best fit for your research. If you are not sure, read the appropriate sections before making your selection.

☒ Life sciences ☐ Behavioural & social sciences ☐ Ecological, evolutionary & environmental sciences

For a reference copy of the document with all sections, see nature.com/documents/nr-reporting-summary-flat.pdf

Life sciences study design

All studies must disclose on these points even when the disclosure is negative.

Sample size	For all experiments, 5 mice were used according to standard scientific conventions, each sample size were described in detail in each figure legend. No statistical methods were used to predetermine the sample size.
Data exclusions	No data were excluded from the analysis.
Replication	For each experiment, at least 4 repeats were done to confirm the reproducibility of the findings and all the replication attempts were successful.
Randomization	Mice of both male and female were used at the same age. And they were randomly assigned to different experiment groups. Only female mice were used in the Pregnancy group and the sham group.
Blinding	For data collection and analysis, the investigators were not blinded to the group allocation. For injury models, the investigators were blinded for group allocation.

Reporting for specific materials, systems and methods

We require information from authors about some types of materials, experimental systems and methods used in many studies. Here, indicate whether each material, system or method listed is relevant to your study. If you are not sure if a list item applies to your research, read the appropriate section before selecting a response.

Materials & experimental systems

n/a	Involved in the study
☐	☒ Antibodies
☒	☐ Eukaryotic cell lines
☒	☐ Palaeontology and archaeology
☐	☒ Animals and other organisms
☒	☐ Human research participants
☒	☐ Clinical data
☒	☐ Dual use research of concern

Methods

n/a	Involved in the study
☒	☐ ChIP-seq
☒	☐ Flow cytometry
☒	☐ MRI-based neuroimaging

Antibodies

Antibodies used	All primary antibodies were commercially available reagents: ZsGreen (Clontech, 632474, 1:1000), Insulin (Dako, A0564, 1:500), Glucagon (Sigma, SAB4501137, 1:500), Somatostatin (Santa Cruz, sc-47707, 1:500), Somatostatin (Abcam, ab-111912, 1:500), Pancreatic polypeptide (Abcam, ab77192, 1:500), Pancreatic polypeptide (Abcam, ab255827, 1:500), E-cadherin (Cell Signaling, 3195, 1:500), Amylase (Sigma, A8273, 1:500), Cytokeratin 19 (Developmental Studies Hybridoma Bank, TROMA-III, 1:200), PDGFRa (R & D, AF1062, 1:500), VE-cadherin (R & D, AF1002, 1:100), Lymphatic vessel endothelial hyaluronan receptor 1 (Abcam, ab14917, 1:500), EdU (Invitrogen, C10338, 1:400), DTR (R & D, AF-259-NA, 1:200), GLUT2 (Abcam, ab54460, 1:500), Nkx6.1 (Abcam, ab221549, 1:500), Pdx1 (Abcam, ab47267, 1:500). After washing, signals were developed with the secondary Alexa fluorescent conjugated antibodies (Invitrogen, 1:1000) for 0.5 hours at room temperature and the cell nuclei were counterstained with DAPI.
Validation	The online methods showed the details about the antibodies. The catalogue number and dilution of each antibodies were included in the online methods, so readers could easily follow the protocol.

Animals and other organisms

Policy information about studies involving animals; ARRIVE guidelines recommended for reporting animal research

Laboratory animals	All mouse experiments were carried out in accordance with the guidelines of the Institutional Animal Care and Use Committee (IACUC) of the Institute of Biochemistry and Cell Biology, and the Institute for Nutritional Sciences, Shanghai Institutes for Biological Sciences, Chinese Academy of Science. Mice were maintained on a C57BL6/ICR mixed background, housed in standard cages and were maintained on a 12-hour light/dark cycle and fed a normal diet.

Wild animals	No wild animals were included in this study.
Field-collected samples	No field-collected samples were included in this study.
Ethics oversight	All mouse experiments were carried out in accordance with the guidelines of the Institutional Animal Care and Use Committee (IACUC) of the Institute of Biochemistry and Cell Biology, and the Institute for Nutritional Sciences, Shanghai Institutes for Biological Sciences, Chinese Academy of Science.

Note that full information on the approval of the study protocol must also be provided in the manuscript.